

AD-A119 839

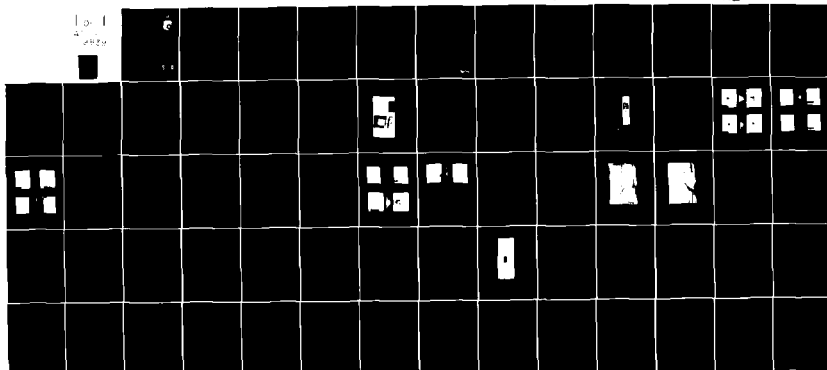
GENERAL ELECTRIC CO CINCINNATI OH AIRCRAFT ENGINE BU--ETC F/B 11/4  
MATERIALS SCREENING TESTS OF THE FOD IMPACT DESIGN TECHNOLOGY P--ETC(11)  
FEB 82 R S BERTKE F33615-77-C-5221

UNCLASSIFIED

AFWAL-TR-82-2043

NL

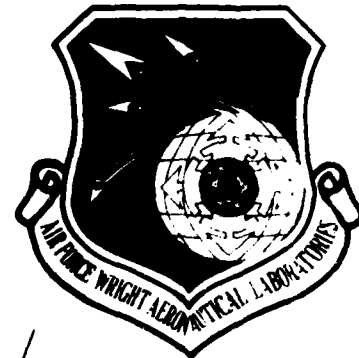
10-1  
4070



END  
DATE  
FILMED  
11 82  
DTIC

7  
12

AFWAL-TR-82-2043



MATERIALS SCREENING TESTS OF THE FOD IMPACT  
DESIGN TECHNOLOGY PROGRAM (TASK IV C)

ROBERT S. BERTKE

University of Dayton Research Institute  
Dayton, Ohio 45469

May 1982

Interim Report for Period 1 October 1977 - 1 June 1980

Approved for public release; distribution unlimited.

DTIC FILE COPY

AERO PROPULSION LABORATORY  
AIR FORCE WRIGHT AERONAUTICAL LABORATORIES  
AIR FORCE SYSTEMS COMMAND  
WRIGHT-PATTERSON AIR FORCE BASE, OHIO 45433

DTIC  
ELECTE  
OCT 4 1982  
S D D

82 10 04 018

NOTICE

When Government drawings, specifications, or other data are used for any purpose other than in connection with a definitely related Government procurement operation, the United States Government thereby incurs no responsibility nor any obligation whatsoever; and the fact that the government may have formulated, furnished, or in any way supplied the said drawings, specifications, or other data, is not to be regarded by implication or otherwise as in any manner licensing the holder or any other person or corporation, or conveying any rights or permission to manufacture, use, or sell any patented invention that may in any way be related thereto.

This report has been reviewed by the Office of Public Affairs (ASD/PA) and is releasable to the National Technical Information Service (NTIS). At NTIS, it will be available to the general public, including foreign nations.

This technical report has been reviewed and is approved for publication.

Sandra K. Drake

SANDRA K. DRAKE  
Project Engineer

Isak J. Gershon

ISAK J. GERSHON  
Technical Area Manager,  
Propulsion Mechanical Design

FOR THE COMMANDER

James M. Shipman

J. SHIPMAN, MAJ, USAF  
Deputy Director, Turbine Engine Division

"If your address has changed, if you wish to be removed from our mailing list, or if the addressee is no longer employed by your organization, please notify AFWAL/PCIA, WPAFB OH 45433 to help us maintain a current mailing list."

Copies of this report should not be returned unless return is required by security considerations, contractual obligations, or notice on a specific document.

UNCLASSIFIED

SECURITY CLASSIFICATION OF THIS PAGE (When Data Entered)

REPORT DOCUMENTATION PAGE		READ INSTRUCTIONS BEFORE COMPLETING FORM
1. REPORT NUMBER AFWAL-TR-82-2043	2. GOVT ACCESSION NO. A119829	RECIPIENT'S CATALOG NUMBER
4. TITLE (and Subtitle) Material Screening Tests of the FOD Impact Design Technology Program (Task IVC)	5. TYPE OF REPORT & PERIOD COVERED Final Tech. Report Oct. 1977 - June 1980	
7. AUTHOR(s) R. S. Bertke	6. PERFORMING ORG. REPORT NUMBER UDR-TR-81-14	
9. PERFORMING ORGANIZATION NAME AND ADDRESS University of Dayton Research Institute 300 College Park Ave. Dayton, Ohio 45469	8. CONTRACT OR GRANT NUMBER(s) 200-4BA-14K-47844 (GE) F33615-77-C-5221	
11. CONTROLLING OFFICE NAME AND ADDRESS General Electric Company Evendale Plant - Aircraft Engine Group Evendale, OH 45215	10. PROGRAM ELEMENT, PROJECT, TASK AREA & WORK UNIT NUMBERS 62203F, 3066, 12, 33	
14. MONITORING AGENCY NAME & ADDRESS (if different from Controlling Office) Aero-Propulsion Laboratory Wright-Patterson Air Force Base Dayton, Ohio 45433	12. REPORT DATE February 1982	
	13. NUMBER OF PAGES 58	
	15. SECURITY CLASS. (of this report) Unclassified	
16. DISTRIBUTION STATEMENT (of this Report)  Approved for public release; distribution unlimited.		
17. DISTRIBUTION STATEMENT (of the abstract entered in Block 20, if different from Report)		
18. SUPPLEMENTARY NOTES		
19. KEY WORDS (Continue on reverse side if necessary and identify by block number) Foreign object damage, screening tests, ballistic limit test, plastic deformation tests, charpy tests, fatigue tests		
20. ABSTRACT (Continue on reverse side if necessary and identify by block number) This report describes a study to develop screening tests to identify and evaluate candidate fan and compressor blade materials of aircraft engines which may possess superior foreign object damage (FOD) resistance. Tests were developed to determine the ballistic limit, local deformation characteristics, gross struc- tural damage characteristics, and the fatigue strength of candi- date blade materials. The data generated demonstrated that the		

DD FORM 1 JAN 73 1473

EDITION OF 1 NOV 65 IS OBSOLETE

UNCLASSIFIED

SECURITY CLASSIFICATION OF THIS PAGE (When Data Entered)

UNCLASSIFIED

SECURITY CLASSIFICATION OF THIS PAGE(When Data Entered)

Screening tests utilized could rate and rank the candidate materials investigated. The materials investigated included 8Al-1Mo-1V and 6Al-4V titaniums, 410 stainless steel in the annealed and heat-treated conditions, a boron/aluminum composite, and a graphite/epoxy composite. Based on the results, the titanium alloys were superior followed by the stainless steel material. The composites showed very poor response to the screening tests and were ranked last.

Equations were developed for each screening tests which can be used to determine the response of new candidate materials to foreign object damage.

UNCLASSIFIED

SECURITY CLASSIFICATION OF THIS PAGE(When Data Entered)

## FOREWORD

This report describes a contractual work effort conducted for the General Electric Company, Aircraft Engine Group under Purchase Order No. 200-4BA-14K-47844 which is a subcontract of F33615-77-C-5221.

This report covers work conducted during the period of October 1977 to June 1980 and is part of Task IV-C.

The GE Program Manager was Mr. Joe McKenzie and the Principal Investigator was Mr. Al Storace. The work reported herein was performed under the direction of Mr. Robert S. Bertke, Impact Physics Group of the Experimental and Applied Mechanics Division, University of Dayton Research Institute.

Technical support was provided by Mr. Charles E. Acton in the study.

This report covers work conducted for project 3066, task 12, entitled Foreign Object Impact Design Criteria. The contract was sponsored by the Aero Propulsion Laboratory, Air Force Systems Command, Wright-Patterson AFB, Ohio 45433 under the direction of Sandra K. Drake (AFWAL/POTA), Project Engineer.

Accession For	
NTIS GRA&I	<input checked="checked" type="checkbox"/>
DTIC TAB	<input type="checkbox"/>
Unannounced	<input type="checkbox"/>
Justification	
By _____	
Distribution/	
Availability Codes	
Dist	Avail and/or Special
A	



# TABLE OF CONTENTS

<u>SECTION</u>		<u>PAGE</u>
I	INTRODUCTION	1
II	WORK PROPOSED	3
	2.1 MATERIALS INVESTIGATED	4
	2.2 SCREENING TESTS	4
	2.2.1 Ballistic Limit Tests	4
	2.2.1.1 Experimental Set-Up	6
	2.2.2 Maximum Deformation Tests	8
	2.2.3 Gross Structural Damage Tests	10
	2.2.3.1 Experimental Set-Up	10
	2.2.4 Fatigue Tests	10
	2.2.4.1 Experimental Set-Up	11
III	EXPERIMENTAL RESULTS	14
	3.1 BALLISTIC LIMIT TESTS	14
	3.1.1 Evaluation of the Ballistic Limit Tests	18
	3.1.2 Technique to Rate Materials to Resistance of Penetration	19
	3.2 PLASTIC DEFORMATION TESTS	20
	3.2.1 Evaluation of the Plastic Deformation Tests	22
	3.2.2 Ranking of Materials to Plastic Deformation Damage	24
	3.3 GROSS STRUCTURAL DAMAGE TESTS	26
	3.3.1 Ranking of the Materials for the Charpy Tests	26
	3.3.2 Evaluation of the Charpy Tests	31
	3.4 FATIGUE TESTING RESULTS	31
	3.4.1 Rating of the Materials for the Fatigue Tests	40
	3.4.2 Evaluation of the Fatigue Test	44
	3.5 OVERALL RANKING OF THE MATERIALS TO THE SCREENING TESTS	44
IV	SUMMARY AND CONCLUSIONS	47
	4.1 BALLISTIC LIMIT TESTS	47
	4.2 PLASTIC DEFORMATION TESTS	48

TABLE OF CONTENTS (CONTINUED)

<u>SECTION</u>	<u>PAGE</u>
4.3 GROSS STRUCTURAL DAMAGE TESTS	49
4.4 FATIGUE TESTS	50
4.5 OVERALL RANKING OF THE MATERIALS TO THE SCREENING TESTS	51
V APPENDIX - TEST RESULTS	52
REFERENCES	58



# LIST OF ILLUSTRATIONS

<u>FIGURE</u>		<u>PAGE</u>
1	Shape of Granite Pebble	5
2	Schematic of Range Set-Up	7
3	Mounting Frame Fixture for Impact Tests	9
4	Typical Composite Specimen with Tabs Installed	13
5	Typical Pebble Impact Damage on 410 SS (Annealed Specimens)	15
6	Typical Pebble Impact Damage on 410 SS (Heat-Treated Specimens)	15
7	Typical Pebble Impact Damage on 8-1-1 Titanium Specimens	16
8	Typical Artificial Bird Impact Damage on 6-4 Titanium Specimens	16
9	Typical Pebble Impact Damage on Boron/Aluminum Composite Specimens	17
10	Typical Artificial Bird Impact Damage on Graphite/Epoxy Composite Specimens	17
11	Typical Plastic Deformation Damage for 8-1-1 Titanium Material	23
12	Typical Plastic Deformation Damage for 410 Stainless Steel Annealed Material	23
13	Typical Plastic Deformation Damage for Boron/ Aluminum Composite Material	24
14	Typical Charpy Impact Test Results on 8-1-1 Titanium Material	27
15	Typical Charpy Impact Test Results on Boron/ Aluminum Material	28
16	Fatigue Results for Graphite/Epoxy Composite Specimens	32
17	Fatigue Results for Boron/Aluminum Composite Specimens	33

LIST OF ILLUSTRATIONS (Continued)

<u>FIGURE</u>		<u>PAGE</u>
18	Fatigue Results for 410 Stainless Steel (Annealed) Specimens	34
19	Fatigue Results for 410 Stainless Steel (Heat-Treated) Specimens	35
20	Fatigue Results for 6-4 Titanium Specimens	36
21	Fatigue Results for 8-1-1 Titanium Specimens	37
22	Longitudinal Cracks Developed on Graphite Epoxy Specimen Upon Dynamic Load Application in Fatigue Testing	39

## LIST OF TABLES

<u>TABLE</u>		<u>PAGE</u>
1	Test Matrix	6
2	Ballistic Limit Velocity Values for the Various Materials	14
3	Ballistic Limit Ranking	20
4	Plastic Deformation Results for Various Materials	21
5	Rating of Materials for Plastic Deformation Damage	25
6	Charpy Test Results	29
7	Charpy Test Average Force and Energy Levels for Each Material	30
8	Rank of Materials to Charpy Tests	31
9	Stress Values of Fatigue Tests at $10^4$ and $10^5$ Cycles for Each Material	41
10	Ranking of Materials for Fatigue Tests	44
11	Rank of the Materials for All the Screening Tests	45

## SECTION I

### INTRODUCTION

Blade damage resulting from the ingestion of foreign objects into gas turbine aircraft engines has to be given serious consideration for reasons of flight safety and costs. Impacts between blades and foreign objects ranging from large birds and ice to small hard particles, such as sand, will almost always cause at least localized minor damage which may be treated as maintenance problems. This resulting damage to the blades may also be severe enough to cause catastrophic failure of an engine which may result in immediate power loss and lead to destruction of the aircraft and crew.

The threat is defined by the environment in which the engine is constrained to operate. The engine speed, blade material, blade geometry, point of impact, and type and size of the impactor all play important roles in determining what type, if any, and the severity of damage which might occur. The blade designers' task is to either design a blade which has a specified level of resistance to foreign object damage (FOD) or to evaluate a given blade and predict the extent of damage to be expected.

The overall design problem has two aspects. The first aspect is a ballistic impact problem. In this instance, a method must be developed to relate the mode and extent of damage to the threat and target parameters. The second aspect of the design problem is to relate the ballistic impact induced damage to the residual properties of the blade. It is the mechanical properties of the blade that are of the most importance or significance in the foreign object damage design problem.

This report describes the results of an experimental program undertaken to develop screening tests to identify and evaluate candidate fan blade materials which may possess superior FOD

resistance. The approach to the investigation was to develop tests to determine the ballistic limit, local deformation characteristics, gross structural damage characteristics, and the residual fatigue strength of candidate blade materials.

## SECTION II

### EXPERIMENTAL PROGRAM

The experimental program involved the development of material screening tests necessary to effectively evaluate and rank candidate materials for fan and compressor blades. It was important that the selected tests would allow simple evaluation of various design concepts, such as the use of thickened sections or stiffeners. It was also desirable to consider screening tests which were relatively small scale, so that expensive testing procedures would not be necessary for material screening.

The scope of the program was to select and develop screening tests that would investigate the material parameters important in the response of blade materials to impact. The material parameters that were investigated in this study include: (a) the perforation resistance of the material; (b) the extent the material may plastically deform; (c) the extent to which the material is vulnerable to catastrophic structural failure; and (d) the extent to which the material is vulnerable to degradation of fatigue properties.

In the investigation, small-scale tests were used to define these material parameters in terms of response to impact. The perforation resistance material parameter was quantified as a ballistic limit velocity ( $V_L$ ) for a given impact condition. The ballistic limit velocity is a direct measure of the amount of impact energy which the material being investigated can absorb without catastrophic local failure. The plastic deformation parameter was quantified by conducting impact tests which maximize the likelihood of plastic deformation. The catastrophic structural failure material parameter was quantified in the instrumented charpy impact test designed to produce gross structural failure. The fatigue properties parameter was quantified in terms of reduction of ultimate fatigue strength of a damaged specimen. The parameters defined by these screening tests was considered individually and also combined for the various materials investigated. In combining the results of the tests, a suitable weighting factor was used to compute an overall figure of merit for a particular material.

## 2.1 MATERIALS INVESTIGATED

The screening tests were used to evaluate and rank six materials. Three of the materials are currently being studied in the overall program. These include 410 stainless steel (in the annealed condition) substituted for the 403 stainless steel used in the J-79 blades, 8Al-1Mo-1V (8-1-1) titanium used in the F-101 blades, and boron/aluminum used in the APSI blades. Additional materials tested in this study include a heat-treated 410 stainless steel, 6Al-4V titanium, and a graphite/epoxy composite. The heat-treated stainless steel was heat-treated to Rockwell C 28 to C 32 condition. All of the titanium specimens were in the shot peened condition to an intensity of 0.005 - 0.008 N using glass beads having 0.023 - 0.033 inch (0.58 - 0.84 mm) diameter.

## 2.2 SCREENING TESTS

The four screening tests utilized in the study include the ballistic limit test, the plastic deformation test, the instrumented charpy impact test, and the fatigue test. Each test and experimental set-up, the test matrix, and the test specimen geometry is described in detail in the following sections.

### 2.2.1 Ballistic Limit Tests

The ballistic limit test involved non-rotating impact test on small test specimens of the six materials using various typical FOD projectiles. In the testing, all of the threat and target parameters are held constant except for the impact velocity. If the impact velocity is then increased from zero, two significant velocities can be identified. The first is the velocity at which the target damage is just detectable. This velocity is denoted ( $V_{th}$ ), the threshold velocity. Above this velocity, the target is measurably damaged. As the velocity is increased above the threshold velocity, target damage increases monotonically. It should be noted that there are various modes of damage in a target, but that each of these modes displays

similar behavior (i.e., above the threshold velocity damage increased with increased velocity). If the velocity is further increased, target perforation will occur. The threat will completely perforate through the target and exit the rear surface with some residual velocity. The velocity at which the threat just perforates the target (i.e., the residual velocity is zero) is designated as the ballistic limit velocity ( $V_L$ ). Above this velocity the threat will perforate the target, while below this velocity the projectile will not perforate the target. The damage reaches a maximum very near to the ballistic limit velocity. As the velocity is increased above the ballistic limit velocity, the damage tends to decline. Finally, at velocities well above the ballistic limit velocity, the damage reaches a constant value independent of velocity. At these velocities the threat perforates the target in the shear plugging mode and a hole is punched in the target with very little peripheral damage. In this test, the determination of the velocity where onset of perforation is initiated was desired.

In the testing, the impact angle was held normal ( $90^\circ$ ) and three impactors were used in the testing. A 0.5 inch (1.27 cm) diameter micro-balloon gelatin sphere with 10 percent porosity was utilized on all six materials. The remaining two impactors were 1.27 cm diameter ice balls and 0.63 cm diameter "standard" pebble. The pebble material was granite which was machined to the cone-cylinder-cone shape shown in Figure 1. The mass of the substitute birds was approximately 0.98 grams, 0.97 grams for the ice balls, and 0.39 grams for the pebbles.

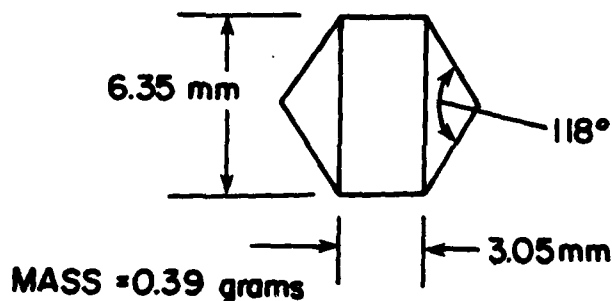


Figure 1. Shape of Granite Pebble



Table 1 summarizes the test conditions conducted for the six materials investigated.

TABLE 1  
TEST MATRIX

Specimen Material	Impact Diameter	Impact Angle
410 Stainless Steel (Annealed)	1.27 cm Bird	90°
	1.27 cm Ice Ball	90°
	0.63 cm Pebble	90°
410 Stainless Steel (Heat Treated)	1.27 cm Bird	90°
	0.63 cm Pebble	90°
8-1-1 Titanium	1.27 cm Bird	90°
	1.27 cm Ice Ball	90°
	0.63 cm Pebble	90°
6Al-4V Titanium	1.27 cm Bird	90°
	1.27 cm Bird	90°
	0.63 cm Pebble	90°
Boron/Aluminum	1.27 cm Bird	90°
	0.63 cm Pebble	90°
Graphite/Epoxy	0.63 cm Bird	90°

#### 2.2.1.1 Experimental Set-Up

A schematic of the range set-up used in the ballistic limit testing is shown in Figure 2. The range set-up consisted of a launch tube, velocity measuring system, sabot catch tank, and a target tank with a mounting fixture. For the 0.63 cm pebble impacts, the launch tube had a smooth bore of 12.7 mm and a length of 1.83 m. The launch tube for the 1.27 cm diameter birds and ice balls was a smooth bore of 20.0 mm having a length of 2.13 m. The projectiles to be fired were positioned into a recessed pocket of a lexan sabot to provide protection and support for the particles during launch. The projectiles/sabot package was launched down the tube by utilizing either compressed gas or powder gas depending on the desired impact velocity. Compressed gas was used for impact velocities up to 305 m/s. Above 305 m/s a powder gun was used. A sabot stopper device was located

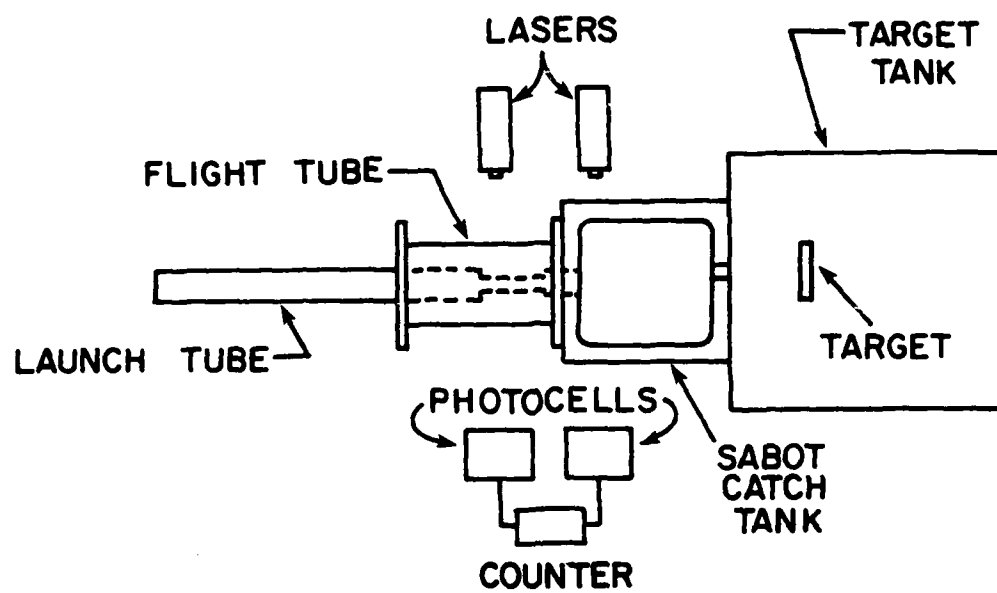


Figure 2. Schematic of Range Set-Up

at the muzzle of the launch tube. The purpose of this device was to slow down and eventually stop the sabot, permitting the projectile to separate from the sabot and continue on trajectory towards the target specimen.

The projectile velocity was measured by utilizing a pair of HeNe laser/photomultiplier stations spaced a known distance apart. Each laser beam intersects the projectile trajectory normal to the trajectory and illuminates one of the photomultiplier stations. When the projectile/sabot package interrupts the first beam (first station had laser beam projecting through slots at muzzle of launch tube), the first photomultiplier station generated a voltage pulse to start a counter-timer. The counter-timer was stopped when the projectiles interrupted the second beam. The projectile velocity was then calculated from the travel time between the stations.

The target specimens for the impact tests were of uniform thickness having a size of 7.62 x 7.62 x 0.152 cm (length, width, and thickness).

All of the target specimens were mounted in a picture frame type fixture for testing as shown in Figure 3. For impact, the specimens were positioned and held by tape such that a 0.48 cm width of each side of the specimen was supported by the mounting fixture.

#### 2.2.2 Maximum Deformation Tests

The identical experimental set-up, mounting procedure, specimen size, etc. that was utilized in ballistic limit tests was used in the maximum plastic deformation tests. In this case, the specimens were impacted by all three projectile types to maximize plastic deformation of the target materials. Again, normal impacts in the specimen center were utilized. The plastic deformation was measured by determining the bulge height on the back surface of the targets. The impact velocity for this testing was slightly below the ballistic limit velocity ( $V_L$ ).

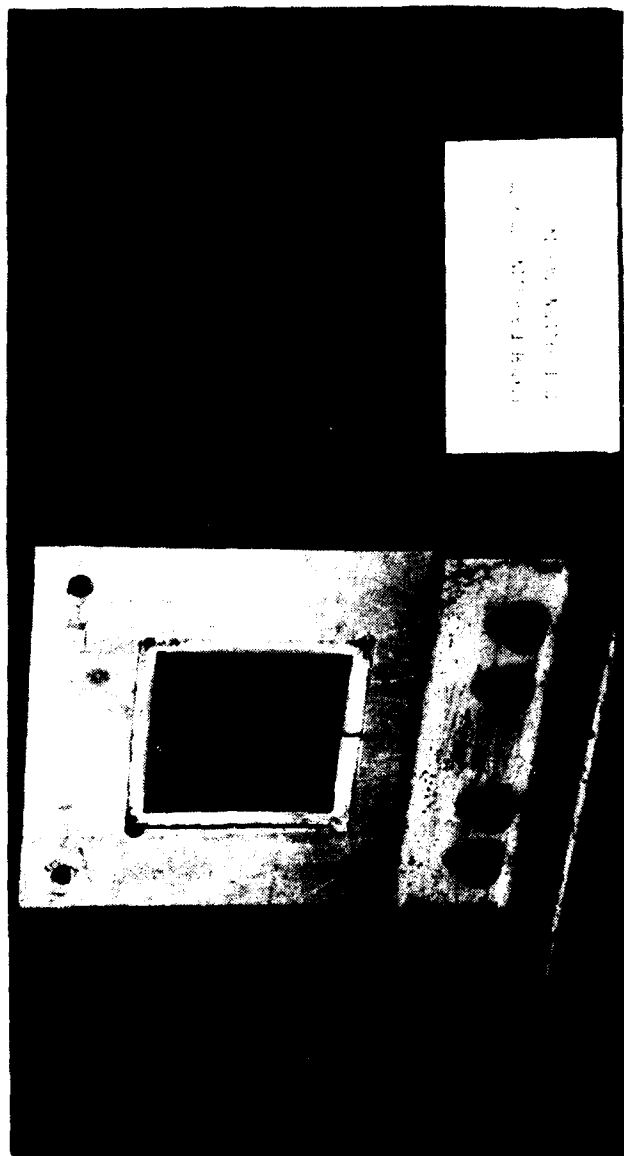


Figure 3. Mounting Frame Fixture for Impact Tests

### 2.2.3 Gross Structural Damage Tests

This test was designed to assess vulnerability to catastrophic structural damage of blades by using test specimens from the six candidate materials. Such damage is probably due to bending stresses at the root or some other mode on an impact blade.

The instrumented charpy impact test was utilized to characterize the material response to bending stresses. The force (S) and energy level required to break a standard thickness specimen were used to rate the six materials investigated.

#### 2.2.3.1 Experimental Set-Up

The instrumented charpy impact tests were conducted on a 217-J (160 ft-lb) Tinius Olsen pendulum impact device instrumented with a Dynatup loading tup and associated electronics from Effects Technology, Inc. Load calibration had previously been performed using standard notched specimens of a rate insensitive aluminum alloy. The pendulum provided an impact velocity of 128 cm/sec which was verified to be accurate to better than 2 percent. This velocity corresponded to 22 J (16.5 ft-lb) of input energy. Load versus time curves were recorded on a storage oscilloscope and photographed. A 5.1 KHz filter in the Dynatup instrumentation was used to filter out high frequency noise and oscillations in the loading tup.

The specimen size used in the charpy tests was 5.72 x 1.00 x 0.15 cm (length, width, and thickness). Since the loading span of the test apparatus is 3.99 cm, a specimen thickness of 0.15 cm gives a slenderness ratio (S/d) of better than 26. Having this high a slenderness ratio assured that the specimens would fail in bending rather than shear (Reference 1).

### 2.2.4 Fatigue Tests

The tensile fatigue strength test was designed to classify damage to specimens in terms of an equivalent stress concentration factor. Either holes or cracks were machined in the center of the specimens at their midspan. The holes were machined by using

drills while the cracks were produced by using the electrical discharge machining technique (EDM) for the metal and the metal-matrix composite specimens. The cracks in the graphite/epoxy composite material was accomplished by using a wire saw.

The machined specimens were tested in a tensile fatigue machine. Each group of specimens with identical damage were tested in the fatigue machine at load levels to obtain failure in the range from  $10^3$  to  $10^5$  cycles. The number of cycles to failure (complete separation) was recorded for each specimen.

#### 2.2.4.1 Experimental Set-Up

The tensile fatigue tests were conducted on either a 2 ton or 6 ton Shenck Resonant Fatigue Testing Machine depending on the necessary tension required to load the various types of specimen materials. The specimens were fatigue tested in tension using a ratio of minimum load to maximum load (R ratio) of 0.1. The cyclic frequency of the Shenck machines was approximately 33 Hz. The number of cycles to failure (complete separation) was recorded for each specimen. No attempt was made to correct for the number of cycles necessary to propagate from the first observable crack or increase in crack length to failure; in all cases this would be small compared to the total cycles. The data for the various specimen materials were plotted as  $N_f$  (number of cycles to failure) versus maximum net section stress.

The specimen size used in tensile fatigue tests was 15.25 x 2.54 x 0.15 cm (length, width, and thickness). Six specimens of each type material had a 0.45 cm diameter hole machined in the chord center of the specimens at their midspan. In addition, six specimens of each type material also had a 0.45 cm long crack centered across the width of the specimens at their midspan.

The composite specimens had 2.54 x 2.54 cm aluminum doubles or tabs added to each end of the specimens such that the grips of the fatigue machine would not directly grip the composite material. Figure 4 shows a typical composite specimen with the tabs installed. The tabs were bonded to the specimens using an adhesive.

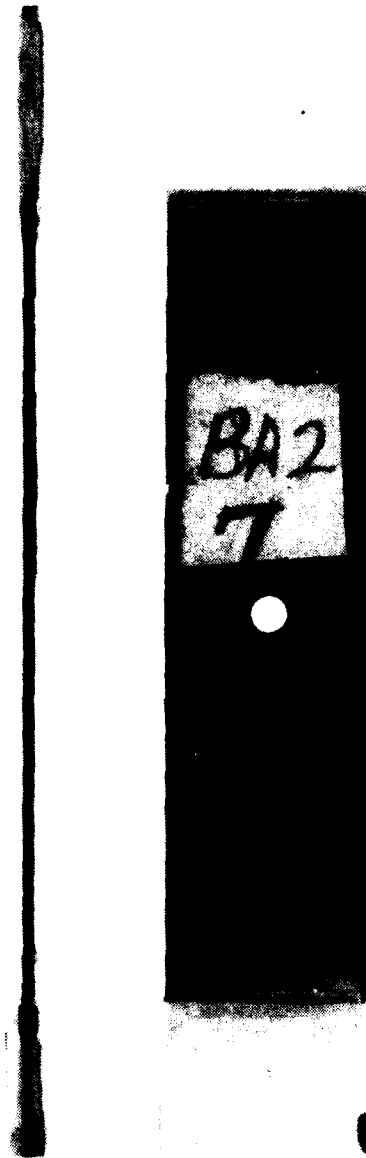


Figure 4. Typical Composite Specimen with  
Tabs Installed



### SECTION III EXPERIMENTAL RESULTS

The experimental results of the various material screening tests conducted to evaluate and rank candidate materials for fan and compressor blading are summarized in the following paragraphs.

#### 3.1 BALLISTIC LIMIT TESTS

The ballistic impact testing consisted of conducting 63 impacts on the six materials investigated. Results of the ballistic limit testing for the three types of impactors are summarized in Table 2. The results indicate that the granite pebble impacts appeared to generate the highest ballistic limit or penetration values. Penetrations were achieved using the granite pebble for all four materials investigated. Typical damage in regards to the ballistic impact tests are shown in Figures 5 through 10 for the six materials investigated. The mode of damage for the metal and boron/aluminum composite specimens when penetration occurred was in the form of either petaling or plugging, while the graphite/epoxy specimens would crack and split through the entire length of the specimens. This mode of damage for the graphite/epoxy material was due to the fact that it was an unidirectional laminate.

TABLE 2  
BALLISTIC LIMIT VELOCITY VALUES FOR  
THE VARIOUS MATERIALS

Target Material	Ballistic Limit Velocity (m/s)		
	Pebble Impacts	Artificial Bird Impacts	Ice Ball Impacts
410 SS (Annealed)	1032	>918	>621
410 SS (Heat Treated)	1017	>596	-
8-1-1 Ti	87	>598	>662
6-4 Ti	-	>586	-
B/Al Composite	193	280	-
G/E Composite	-	97	-



Figure 5. Typical Pebble Impact Damage on 410 SS (Annealed Specimens)



Figure 6. Typical Pebble Impact Damage on 410 SS (Heat Treated Specimens)



Figure 7. Typical Pebble Impact Damage on 8-1-1 Titanium Specimens

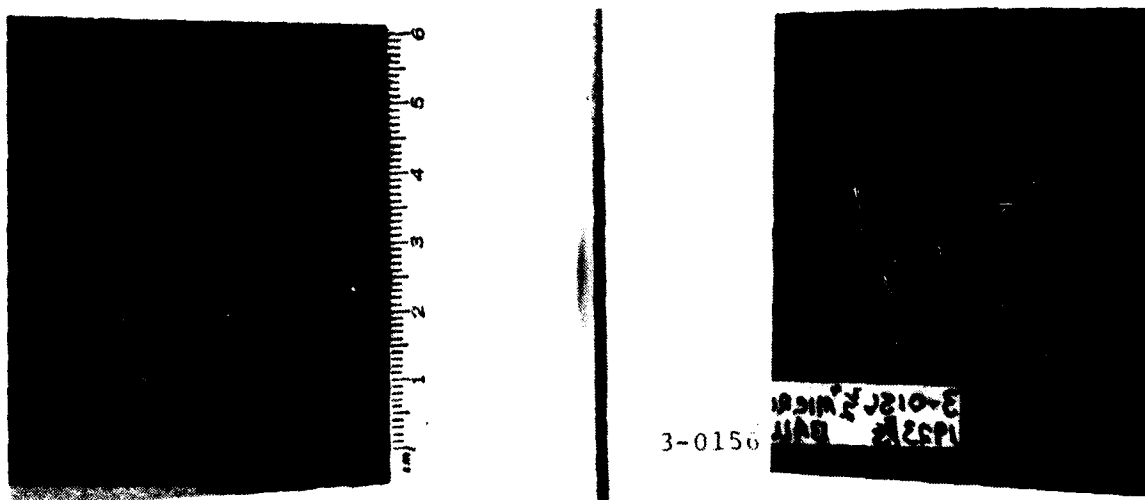


Figure 8. Typical Artificial Bird Impact Damage on 6-4 Titanium Specimens

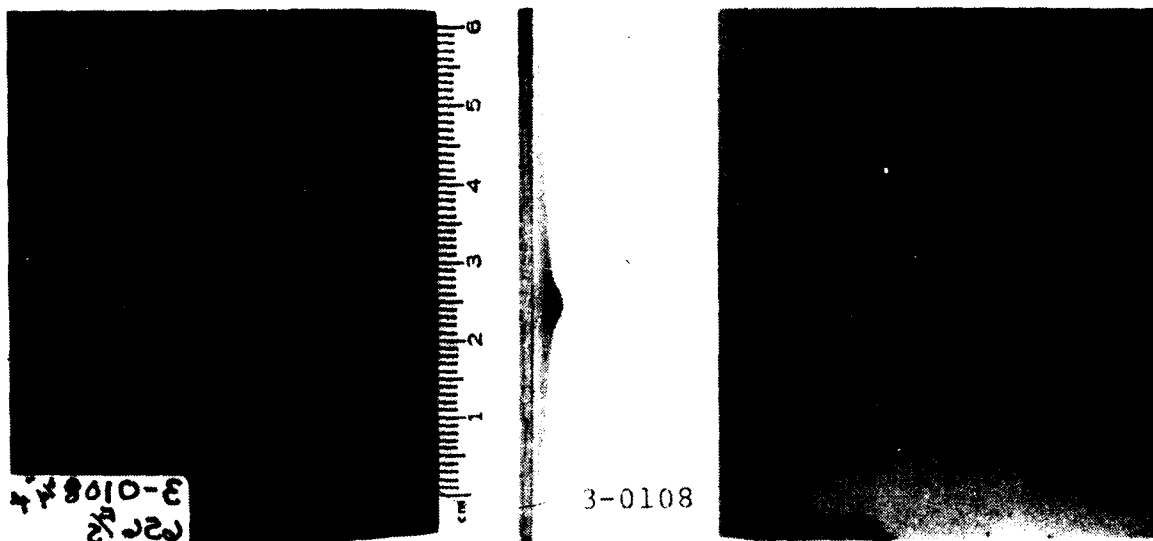


Figure 9. Typical Pebble Impact Damage on Boron/Aluminum Composite Specimens

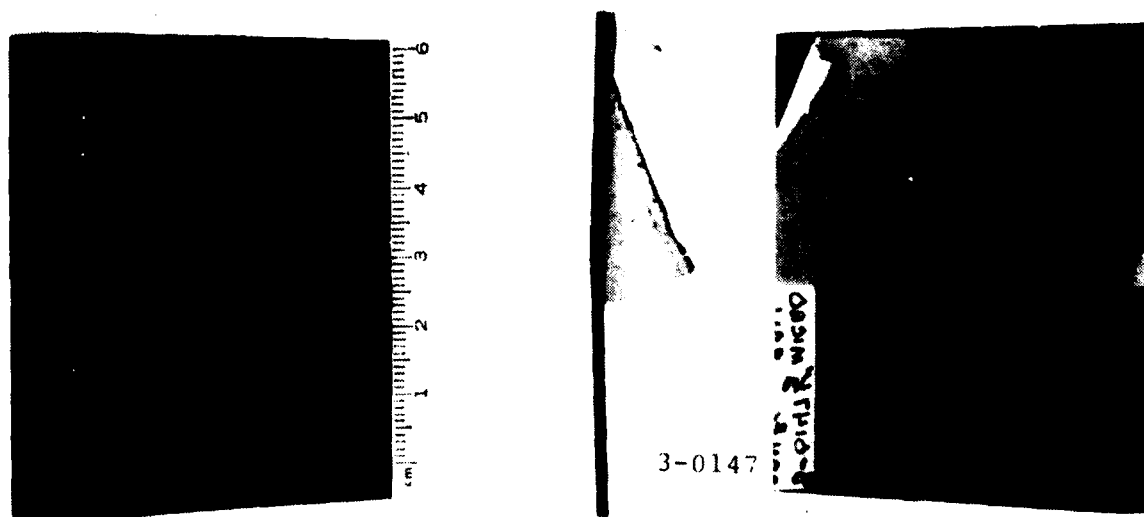


Figure 10. Typical Artificial Bird Impact Damage on Graphite/Epoxy Composite Specimens

Ranking the materials investigated, the 410 SS material appears to give the best level of resistance to penetration followed by the titanium material for the pebble impacts. From the results of the testing, the stainless steel annealed and heat-treated material has a ballistic limit velocity of approximately 1020 m/s whereas the titanium material has a ballistic limit velocity of about 870 m/s for the granite pebble impacts. The ballistic limit velocity for the boron/aluminum material was very low at 193 m/s compared to the metal materials for the pebble impacts.

For the micro-balloon gelatin impacts, no penetrations could be achieved on the metal materials while penetration occurred at 280 m/s for the boron/aluminum material and 97 m/s for the graphite/epoxy material. No attempt was made to launch the artificial birds to velocities greater than 600 to 900 m/s because of the acceleration forces on launching the soft body projectiles in the launch tubes. At the high velocities, the birds would break up before leaving the muzzle of the launch system. It was also discovered that launching ice balls above about 640 m/s would result in the ice breaking up during the launch.

The ice ball impacts on the two metal materials up to 640 m/s resulted in non-penetrations.

Data for the various ballistic impacts are collected in Appendix A.

#### 3.1.1 Evaluation of the Ballistic Limit Tests

For the three projectile types used in the ballistic limit tests, only the pebble impacts generated perforations on all of the materials they were tested on. Except for the composite materials, non-penetrations were received on the metal materials from the artificial bird and ice ball impacts. The launch velocities of the artificial birds and the ice balls was limited to prevent projectile break-up during the

launch. Thus, the pebble impacts are the only ones which gave meaningful data from which a ranking of the materials could be conducted. The non-perforations received from the artificial bird and ice ball impacts on the metal specimens support the validity for using only the pebble data.

Careful considerations must be made in selecting the projectile types when using the ballistic limit tests as a screening test to evaluate candidate materials for FOD damage such that penetrations or perforations are received on the specimens.

### 3.1.2 Technique to Rate Materials to Resistance of Penetration

The ballistic limit velocity of the pebble impacts was used to rank the various materials investigated. The material with the highest ballistic limit velocity was given a ranking value of ten. The best material appeared to be the stainless steel specimens with both the annealed and heat-treated conditions having a similar ballistic limit velocity of 1020 m/s. The ballistic limit velocities for each of the materials was then determined by the equation:

$$V_1 = \frac{\text{material ballistic limit}}{1020} \times 10.$$

Using this system to rank the materials in regards to resistance to penetration, Table 3 gives the rank of the various materials. The best material was the stainless steel in either the annealed or heat-treated conditions with a ranking of 10.0. The 8-1-1 Ti was the next best with a ranking of 8.5. Although, the 6-4 Ti was not impacted by pebbles, it was given the same rank of 8.5 as for the 8-1-1 Ti. The mechanical properties of both titanium alloys are very similar and it was felt that the ballistic limit results would be similar. The boron/aluminum had a ranking of 1.9 which is the lowest of materials investigated by pebble impacts. It is felt; however, that the graphite/epoxy would

even have a lower rank than the boron/aluminum if pebble impacts had been conducted on this material. The reason is that the ballistic limit for the graphite/epoxy was only 97 m/s compared to 280 m/s for the boron/aluminum material for the artificial bird impacts. A ranking of about 0.7 was calculated by multiplying the ranking for the boron/aluminum by the ratio of the ballistic limit for the graphite/epoxy to that of the boron/aluminum material for the artificial bird impacts.

### 3.2 PLASTIC DEFORMATION TESTS

The plastic deformation tests consisted of impacting the specimens with the projectiles to maximize plastic deformation of the six materials investigated. As in the ballistic limit tests, normal impacts in the specimen center were utilized. Table 4 gives the average deformation results for the three types of projectile impacts. Again, the limited velocities that the artificial bird and ice balls could be fired without projectile breakup within the launch tube generated plastic deformation damage which is not at its maximum except for the

TABLE 3  
BALLISTIC LIMIT RANKING

Target Material	Pebble Impacts
410 SS (Annealed)	10.0
410 SS (Heat Treated)	10.0
8-1-1 Ti	8.5
6-4 Ti	~8.5
B/Al Composite	1.9
G/E Composite	~0.7

TABLE 4  
PLASTIC DEFORMATION RESULTS  
FOR VARIOUS MATERIALS

Test Material	Pebble Impacts		Artificial Bird Impacts		Ice Ball Impacts	
	Velocity (m/s)	Plastic Deformation (mm)	Velocity (m/s)	Plastic Deformation (mm)	Velocity (m/s)	Plastic Deformation (mm)
8-1-1 Ti	855	3.60	589	2.28	618	0.42
6-4 Ti	---	---	586	2.81	---	---
410 SS (Annealed)	1001	11.50	637	5.00	613	3.56
410 SS (Heat Treated)	941	7.80	595	3.14	---	---
Boron/Aluminum	182	2.20	227	2.62	---	---
Graphite/Epoxy	---	---	97	No Plastic Deformation	---	---



composite specimens. Therefore, the pebble impacts generated the only meaningful data in the testing. Based on the pebble impacts, the results show that the 410 stainless steel material in the annealed condition had the highest plastic deformation value. An average deformation of 11.5 mm was received for pebble impacts at an average velocity of 100 m/s. The 410 stainless steel specimens had an average plastic deformation value of 7.8 mm for an average velocity of 941 m/s. The best material in regards to plastic deformation appeared to be the 8-1-1 titanium with an average value of 3.6 mm at an average velocity of 855 m/s. For the pebble impacts, the boron/aluminum material had the least plastic deformation of 2.2 mm; however, the velocity was very low at 182 m/s.

The maximum plastic deformation for the artificial bird impacts on the boron/aluminum materials was 2.62 mm at a velocity of 227 m/s. The graphite/epoxy exhibited no measurable plastic deformation up to its ballistic limit velocity of 97 m/s for the artificial bird impacts. Typical damage in regards to plastic deformation is shown in Figures 11 through 13.

#### 3.2.1 Evaluation of the Plastic Deformation Tests

For the three projectile types used in the plastic deformation tests, only the pebble impacts generated maximum plastic deformation on the metal specimen materials investigated. These maximum deformations were received at velocities which were slightly below the ballistic limit velocities for each materials investigated by pebble impacts. Data of the artificial bird and ice ball impacts is meaningful for the composite materials; however, it is not for the metal materials because of the velocity limitation to prevent break-up of the projectiles in the launch tube. Therefore, careful considerations must be made in selecting the projectile types when using the plastic deformation tests as a screening test to evaluate candidate materials.

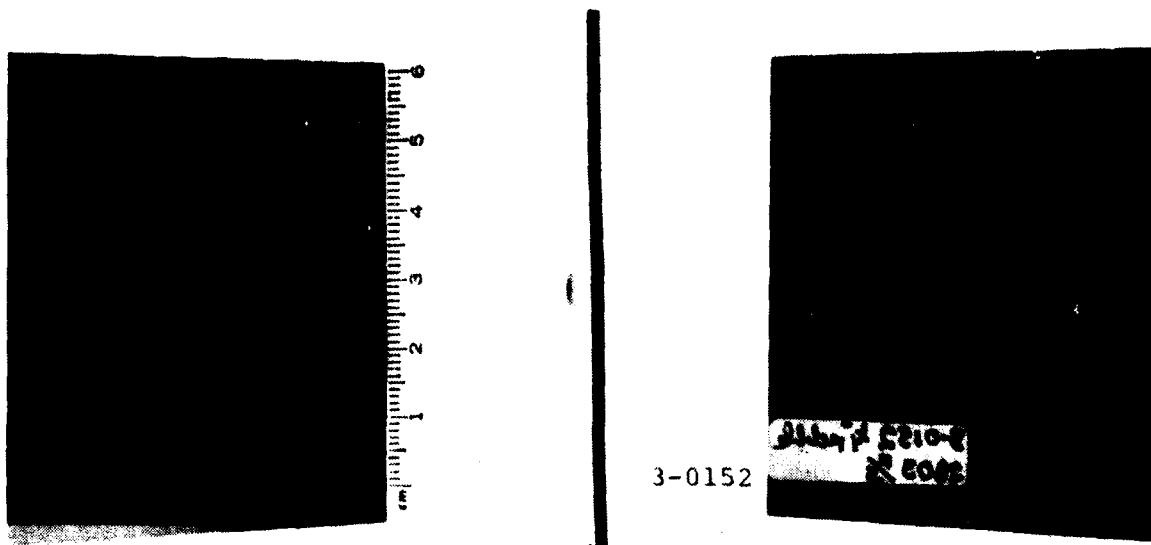


Figure 11. Typical Plastic Deformation Damage for 8-1-1 Titanium Material



Figure 12. Typical Plastic Deformation Damage for 410 Stainless Steel Annealed Material

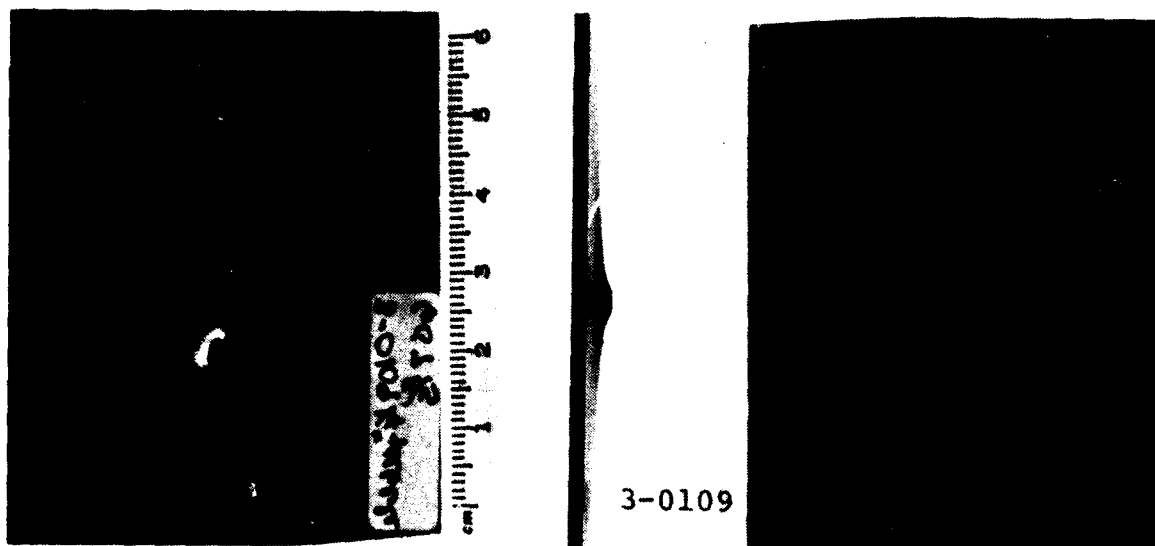


Figure 13. Typical Plastic Deformation Damage for Boron/  
Aluminum Composite Material

### 3.2.2 Ranking of Materials to Plastic Deformation Damage

A slight amount of plastic deformation may be considered relatively benign; however, a large amount of plastic deformation (which changes the blade shape) can effect the aerodynamic performance of fan blades that pump air through the engine in an efficient manner. A second effect of plastic deformation on aerodynamic performance is to change the angle of attack of the blade. This change in angle of attack may be due to either local or global twisting or bending of the blade. Such changes in angle of attack can significantly affect subsequent pumping efficiency. It is also possible that a combination of elastic and plastic deformation of a blade may be sufficiently large enough to impact static structural components of the engine located close to the rotor stage and cause catastrophic failure of the blade and engine.

The impact velocity has to be taken into consideration when rating the various materials for maximum plastic

deformation damage. The best material appeared to be the 8-1-1 titanium with plastic deformation of 3.6 mm for an average pebble velocity of 855 m/s and was assigned a rating of ten. The remaining materials were rated by using the data for the 8-1-1 titanium. The equation for rating the materials is:

$$PD_R = \frac{\text{material impact velocity}}{\text{plastic deformation}} \times \frac{3.6}{855} \times 10.$$

Using this system to rate each material to plastic deformation resistance, Table 5 gives the ratings. Although, the 6-4 titanium material was not impacted by pebbles, it was given the same rating of 10.0 as for the 8-1-1 titanium. The mechanical properties of both titanium alloys are very similar; therefore, it was assumed that the plastic deformation damage would be similar. The 410 stainless steel in the heat-treated condition has a rating of 5.1 while the annealed alloy is rated considerably less at 3.7. Although the boron/aluminum material has the lowest plastic deformation damage for pebble impacts, the velocity was also the lowest at 182 m/s. Considering this low velocity with the plastic deformation, a rating of 3.4 was calculated using the equation. The composite of graphite/epoxy was very brittle and showed no plastic deformation for the substitute bird impacts; however, the impact velocity was very low at 97 m/s. In this case, only the ratio of the velocities was used to give a rating of 1.1.

TABLE 5  
RATING OF MATERIALS FOR PLASTIC DEFORMATION DAMAGE

Target Material	Rating
8-1-1 Titanium	10.0
6-4 Titanium	10.0
410 SS (Heat Treated)	5.1
410 SS (Annealed)	3.7
Graphite/Epoxy	1.1
Boron/Aluminum	3.4

### 3.3 GROSS STRUCTURAL DAMAGE TESTS

The instrumented charpy impact test was utilized to characterize the material response of the six materials to bending stresses. The force and energy level required to break a standard thickness specimen was used to rate the materials. The tests were conducted on a Tinius Olsen pendulum impact machine instrumented with a Dynatup loading tup and associated electronics. Prior to testing, specimen dimensions were measured for all specimens. Load versus time and energy versus time curves were recorded on a storage scope and photographed. Typical records for 8-1-1 titanium and boron/aluminum are shown in Figures 14 and 15 respectively. The load setting for Figure 14 was 50 pounds per division while the energy setting was 5 foot-pounds per division. The time setting was 5 mil-seconds per division. The bottom trace represents the load while the top trace gives the energy. The load settings for Figure 15 (boron/aluminum specimen) was 25 pounds per division while the energy setting was 0.5 foot-pounds per division. The time setting for the boron/aluminum material was 0.5 mil-seconds per division. Notice that a substantial amount of yielding was experienced for the metal specimens and very little for the composite specimen. The composite specimens would fail almost instantly without yielding once the peak force was reached.

Table 6 gives the results of the charpy impact tests for the individual specimens. The peak force (pounds) and peak energy (foot-pounds) were calculated from the oscilloscope traces. The energy must be corrected to account for the reduction in the pendulum velocity as a result of the impact with the sample. The last column of Table 5 gives the corrected energy (foot-pounds which takes into account this reduction of velocity).

#### 3.3.1 Ranking of the Materials for the Charpy Tests

The ranking of the materials was achieved by calculating the average peak force and peak energy levels of

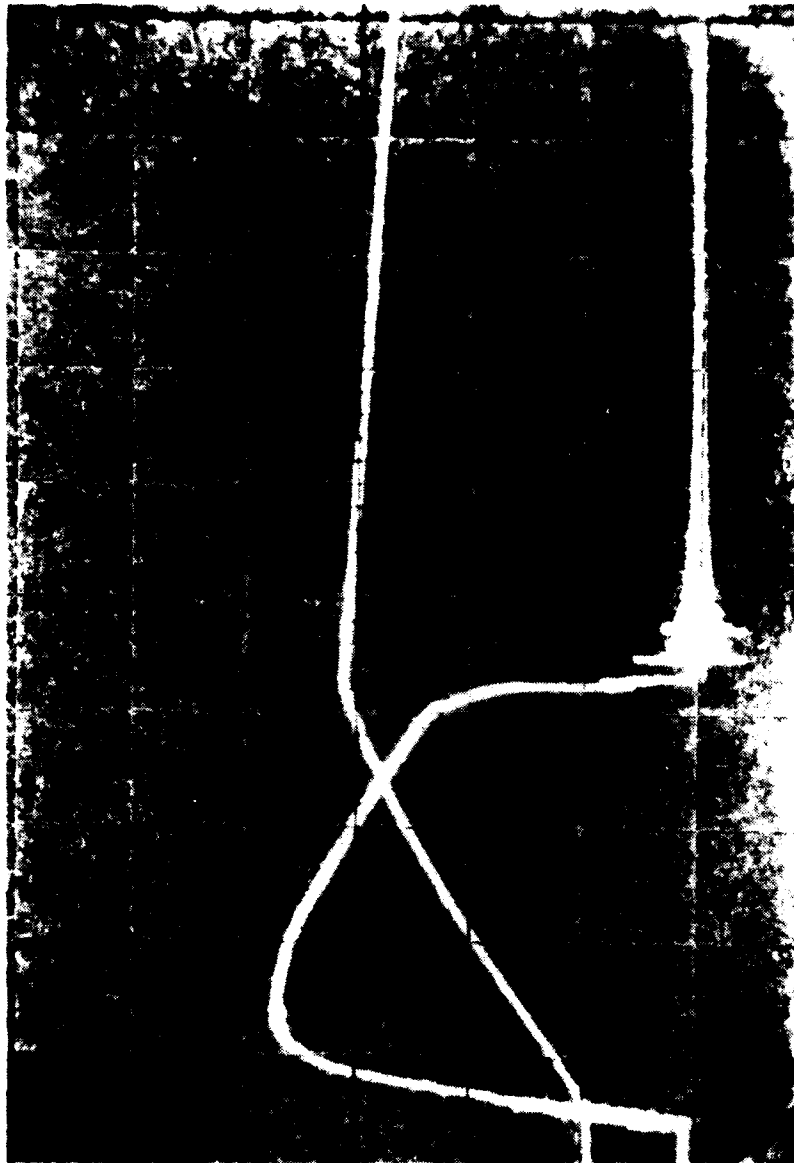


Figure 14. Typical Charpy Impact Test Results on  
8-1-1 Titanium Material

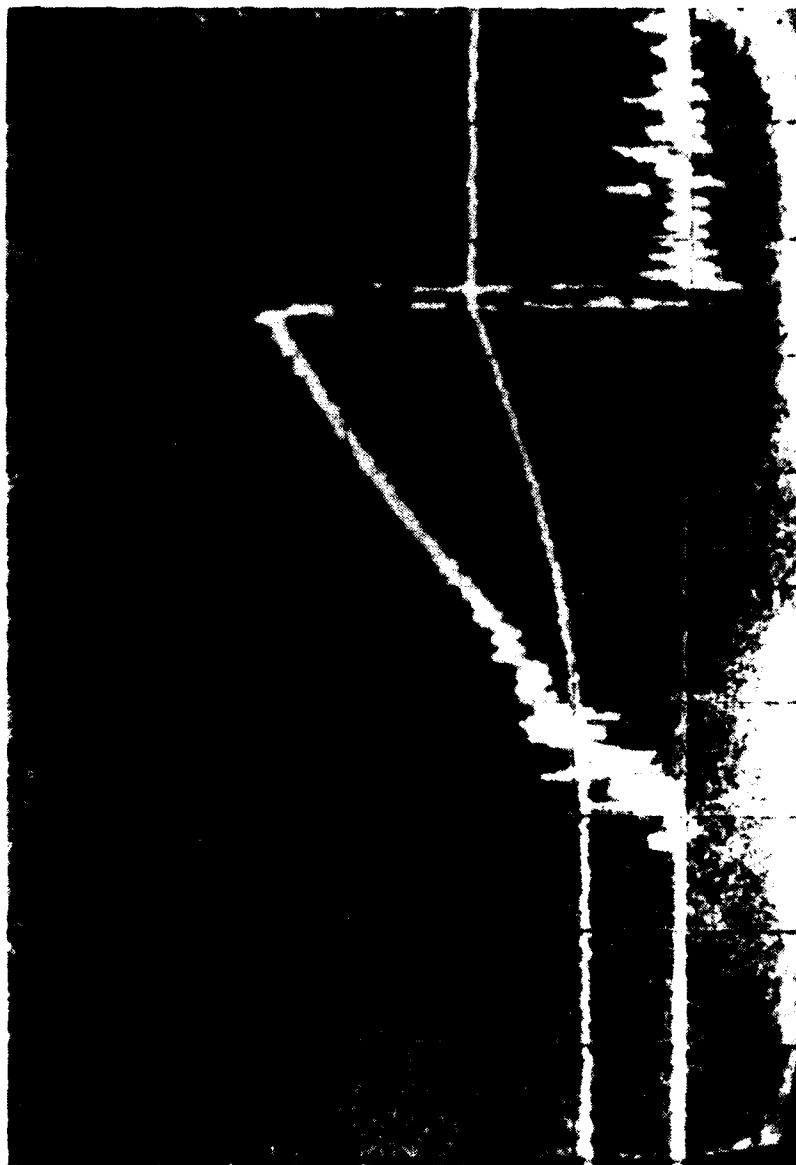


Figure 15. Typical Charpy Impact Test Results on Boron/Aluminum Material

TABLE 6  
CHARPY TEST RESULTS

Material	Specimen Number	Peak Force (lbs)	Corrected Peak Energy (ft-lbs)
8-1-1 Ti	1	180.6	8.6
8-1-1 Ti	2	183.6	9.1
8-1-1 Ti	3	180.6	9.1
8-1-1 Ti	4	188.1	9.2
6-4 Ti	1	167.2	8.1
6-4 Ti	2	167.2	8.3
6-4 Ti	3	164.2	7.8
6-4 Ti	4	165.7	8.1
410 SS (Annealed)	1	77.6	4.0
410 SS (Annealed)	2	79.1	4.0
410 SS (Annealed)	3	76.1	3.9
410 SS (Annealed)	4	76.1	3.9
410 SS (Heat Treated)	1	153.7	7.9
410 SS (Heat Treated)	2	153.7	7.8
410 SS (Heat Treated)	3	149.3	7.7
410 SS (Heat Treated)	4	149.3	7.6
Boron/Aluminum	C-1D	85.1	0.45
Boron/Aluminum	C-1E	88.1	0.51
Boron/Aluminum	C-2E	92.5	0.51
Boron/Aluminum	3D	89.6	0.51
Boron/Aluminum	C-3D	87.3	0.43
Graphite/Epoxy	BA-3-A	148.5	0.86
Graphite/Epoxy	BA-3-B	150.0	0.96
Graphite/Epoxy	BA-3-D	128.6	0.69
Graphite/Epoxy	BA-3-C	134.3	0.77



Table 6 for all the materials as given in Table 7 and then dividing each of the average values by the average value for the best material which was 8-1-1 titanium. Based on the results, the 8-1-1 titanium was given a ranking of ten for a force of 183.2 pounds and a peak energy of 9.00 foot-pounds. The results of the other materials were then normalized by using the equations:

$$\text{Force} = \frac{\text{force of material}}{183.2} \times 10$$

for the peak force and:

$$\text{Peak Energy} = \frac{\text{energy of material}}{9.00} \times 10$$

for the peak energy level. Using this system to rate the materials, Table 8 gives the rank of the various materials for the peak force and energy values.

The resulting peak force and energy rank values were then averaged to give an overall ranking of the materials which is given in the third column of Table 8. Using this method, the 8-1-1 titanium material was the best material with a rank of ten followed by the 6-4 titanium with a rank of 9.05. The 410 stainless steel in the heat-treated condition has a rank of 8.75 followed by the graphite/epoxy and annealed stainless steel materials with a rank of 4.3. The worst material was the boron/aluminum with rating of 2.65

TABLE 7  
CHARPY TEST AVERAGE FORCE AND  
ENERGY LEVELS FOR EACH MATERIAL

Material	Force (lbs)	Peak Energy (ft-lbs)
8-1-1 Ti	183.2	9.00
6-4 Ti	166.1	8.10
410 SS (Annealed)	77.2	4.00
410 SS (Heat Treated)	151.5	7.80
Boron/Aluminum	88.5	0.48
Graphite/Epoxy	140.4	0.82

TABLE 8  
RANK OF MATERIALS TO CHARPY TESTS

Test Material	Peak Force Ranking	Peak Energy Ranking	Overall Average
8-1-1 Ti	10.0	10.0	10.00
6-4 Ti	9.1	9.0	9.05
410 SS (Annealed)	4.2	4.4	4.30
410 SS (Heat Treated)	8.3	9.2	8.75
Boron/Aluminum	4.8	0.5	2.65
Graphite/Epoxy	7.7	0.9	4.30

### 3.3.2 Evaluation of the Charpy Tests

It is felt that the charpy test is a very important test when gross structural damage such as bending at the root and gross local bending is involved at the impact site for FOD impacts. This screening test appears to be an excellent test to measure the response of the materials to bending.

### 3.4 FATIGUE TESTING RESULTS

The machined damage (either holes or cracks) were fatigue tested in tension on either a 2 ton or a 6 ton Shenck Resonant Fatigue Testing Machine depending on the necessary tensile level required to load the various types of specimen materials. The ratio of minimum load to maximum load (R ratio) utilized in the testing was 0.1. The number of cycles to failure (complete separation) was recorded for each specimen. No attempt was made to correct from the first observable crack or increase in crack length to failure except for the graphite/epoxy specimens. The data for the various specimen materials were plotted as  $N_f$  (number of cycles to failure) versus maximum net section stress.

Figures 16 through 21 shows the results of the testing for the various materials tested. Figure 16 shows the fatigue results for the graphite/epoxy composite. The results show that



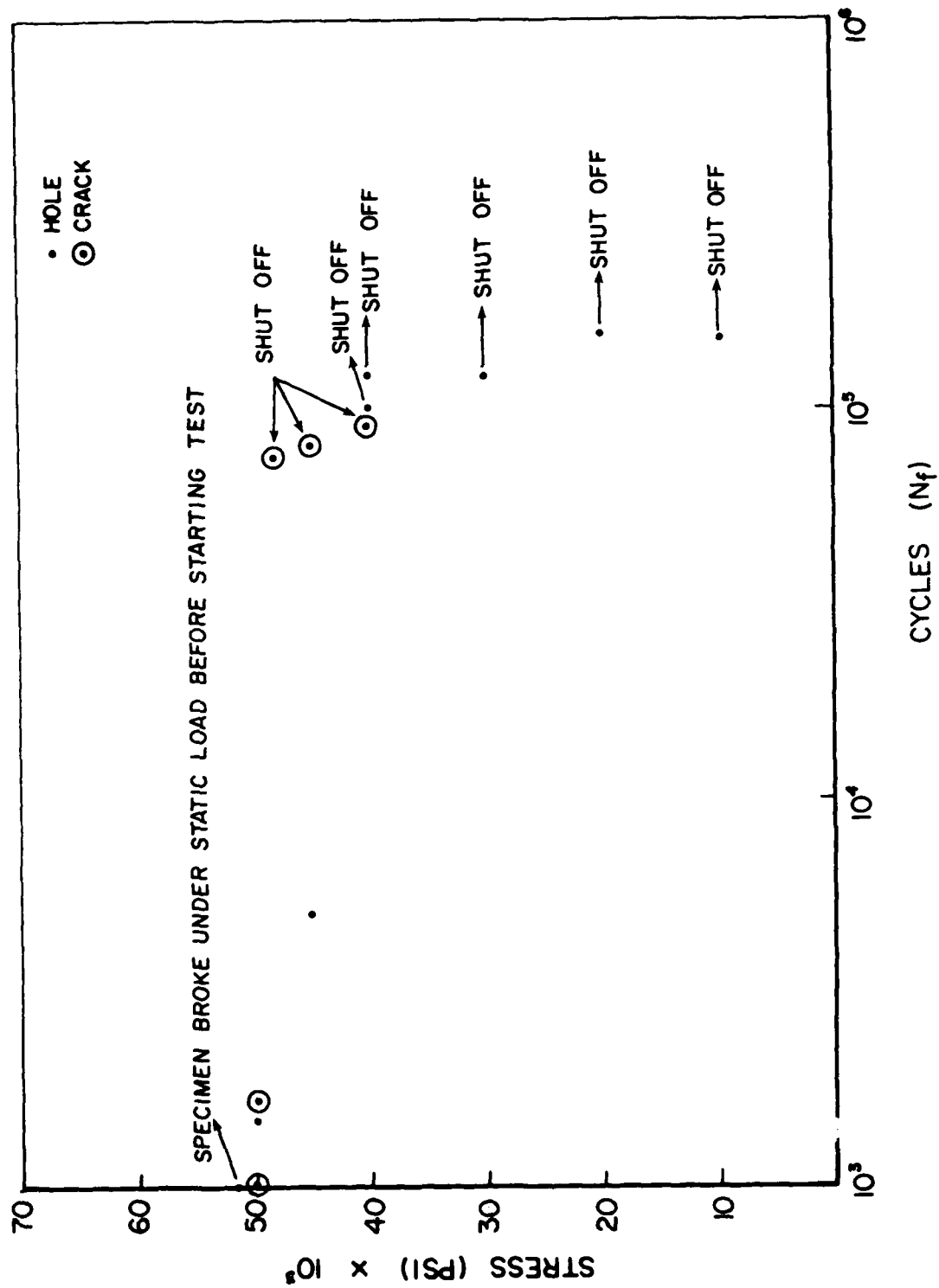


Figure 17. Fatigue Results for Boron/Aluminum Composite Specimens

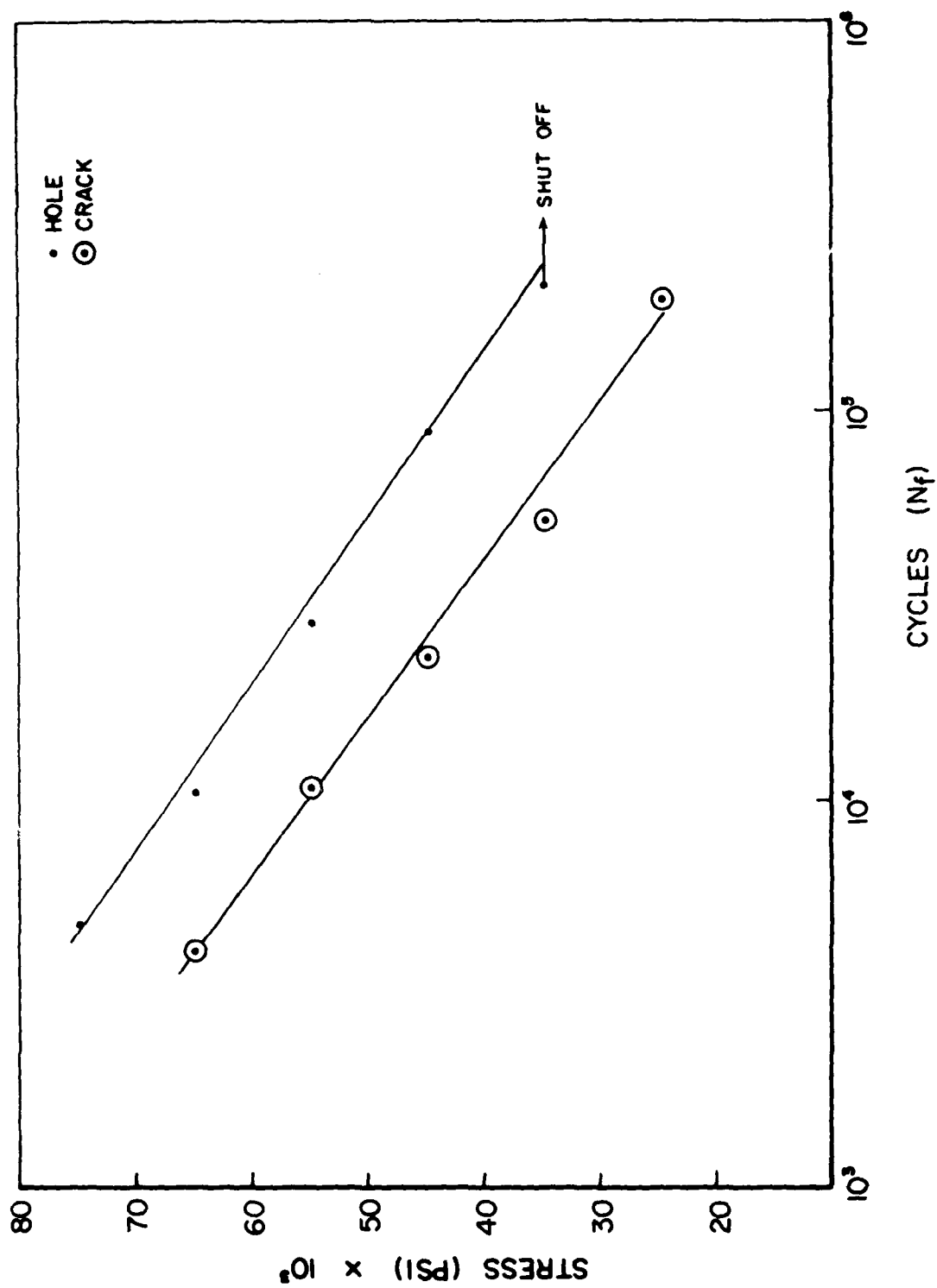


Figure 18. Fatigue Results for 410 Stainless Steel (Annealed) Specimens

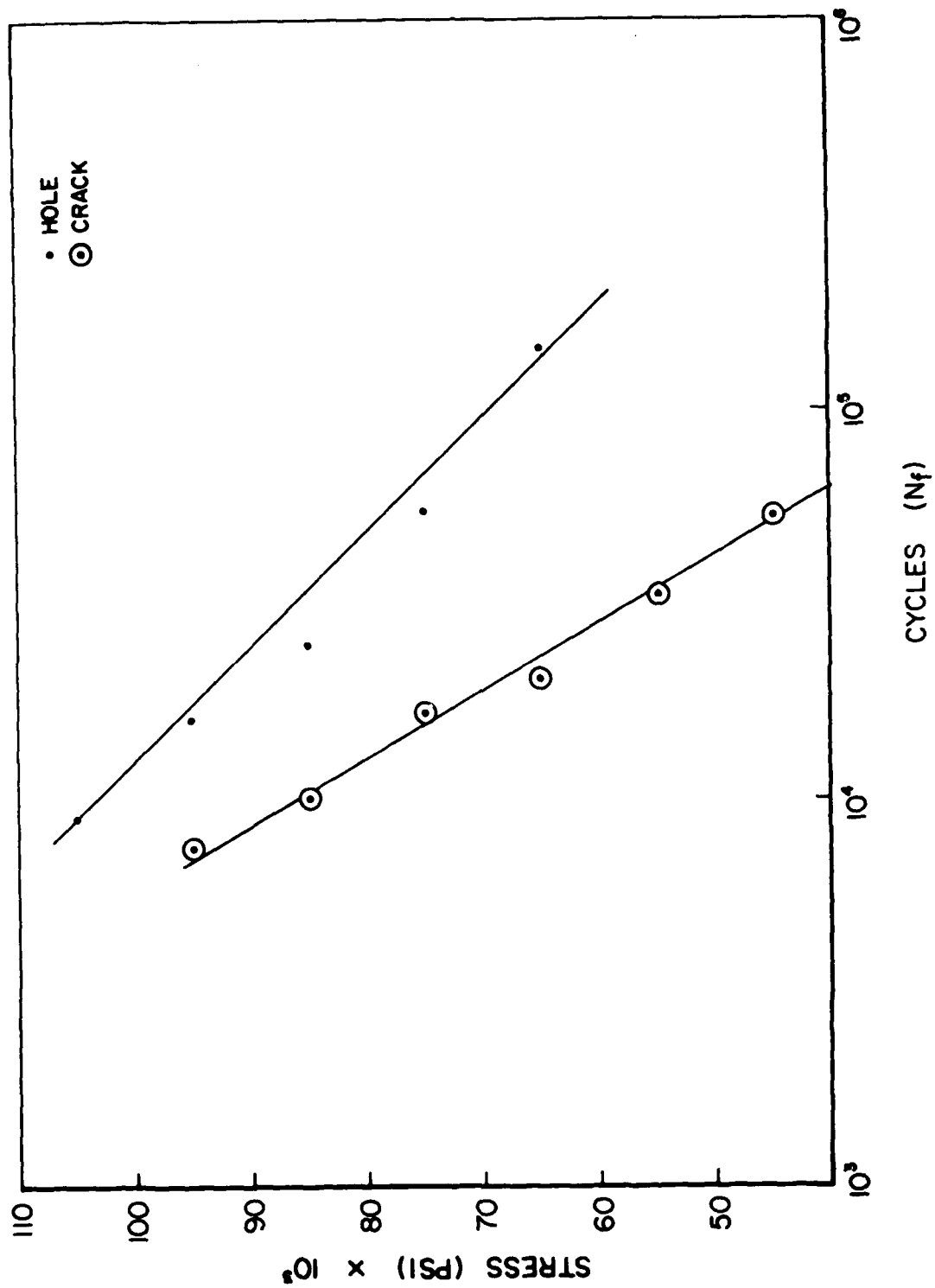


Figure 19. Fatigue Results for 410 Stainless Steel (Heat Treated) Specimens

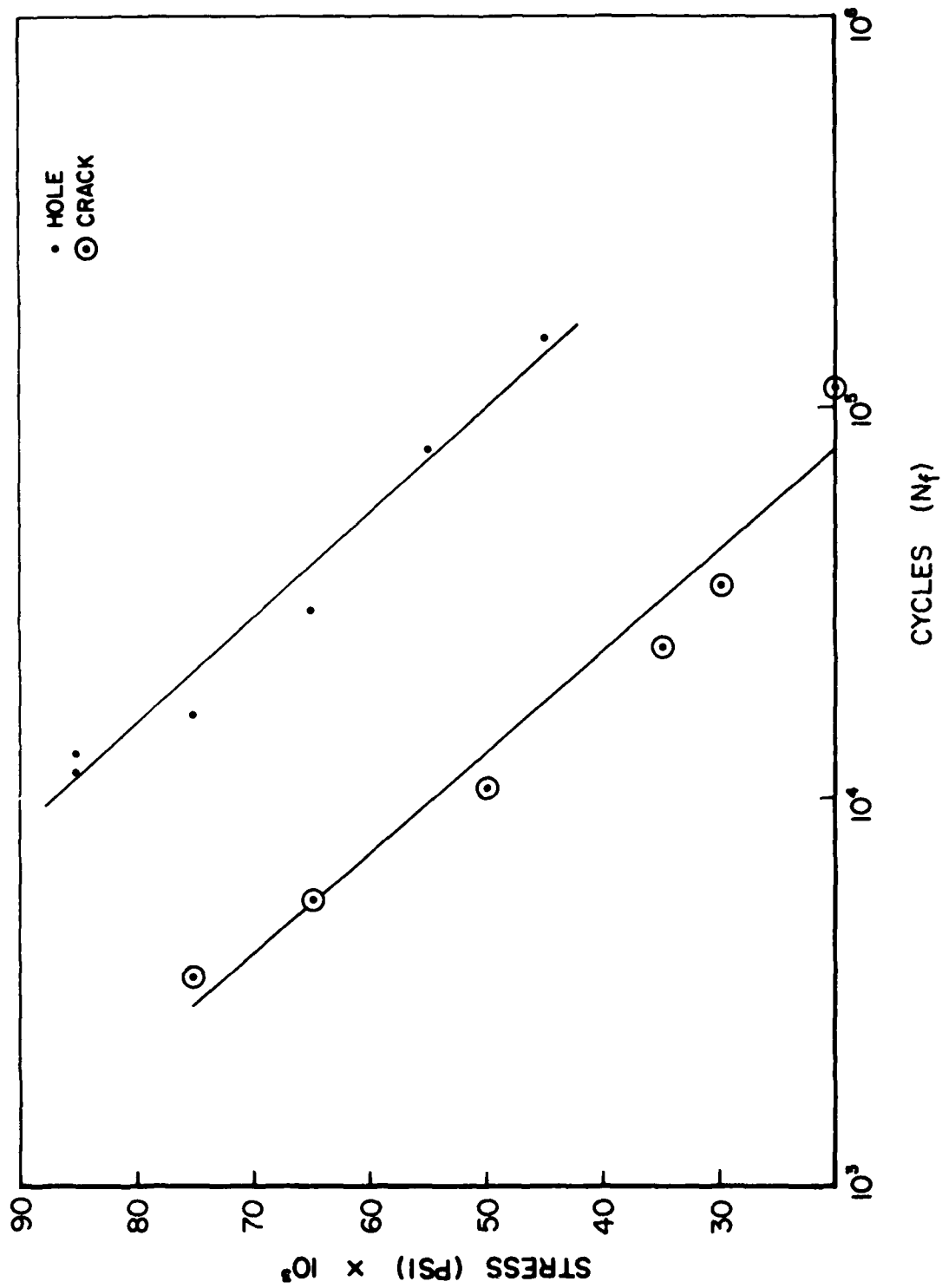


Figure 20. Fatigue Results for 6-4 Titanium Specimens

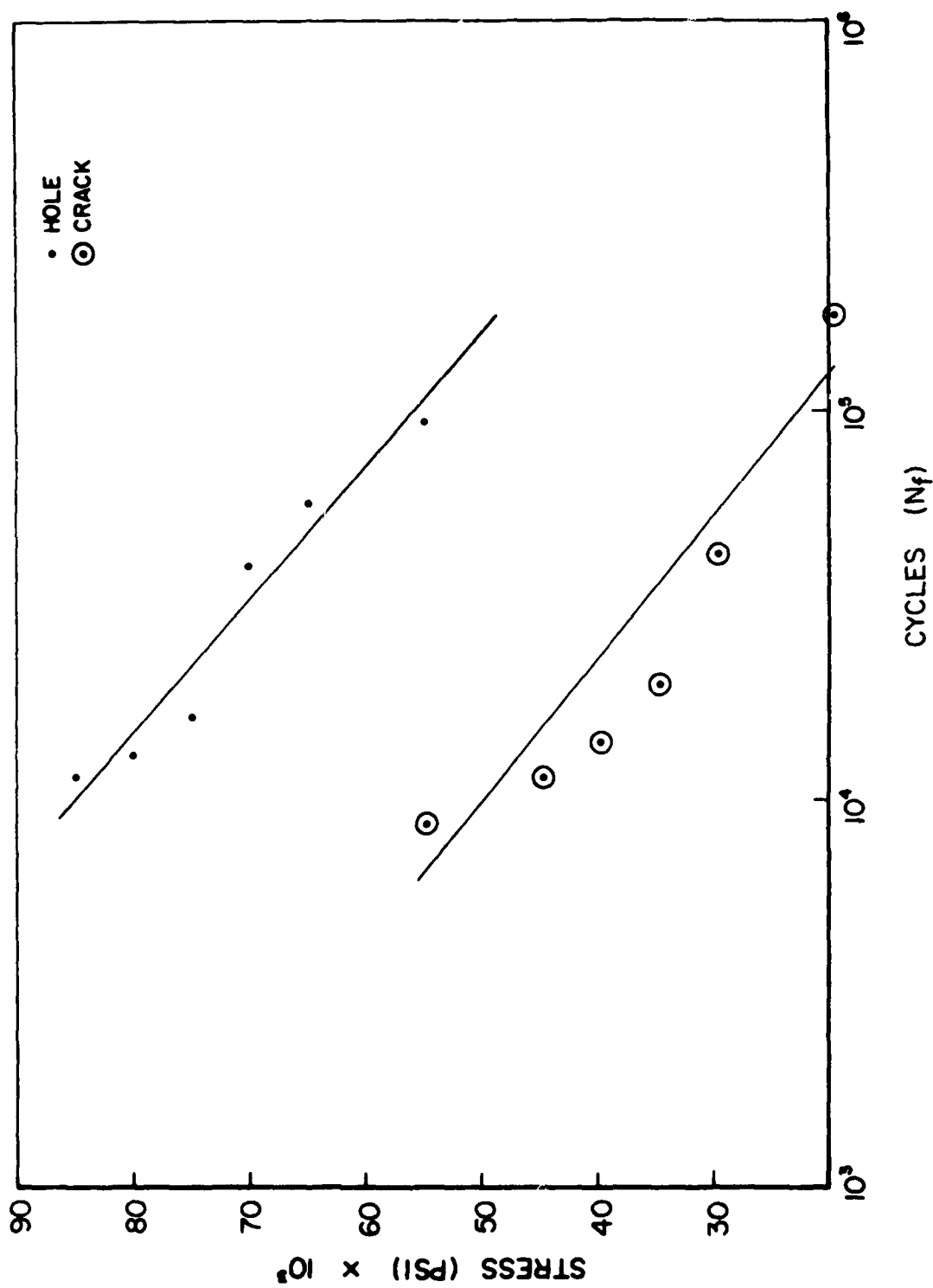


Figure 21. Fatigue Results for 8-1-1 Titanium Specimens



the endurance limit at  $10^5$  cycles is above 70 ksi for the graphite/epoxy material. On the specimens with machined cracks, longitudinal cracks occurred when the dynamic load was applied and these cracks continued to grow until the test was stopped. The tests on the machined hole specimens was stopped when cracks became visible which ran across the width dimension of the specimens. Figure 22 shows these longitudinal cracks on a typical graphite/epoxy specimen.

The stress concentration factor ( $K_t$ ) for the axial loading case of a finite width plate with the transverse hole was 2.55 for all the materials<sup>(2)</sup>.

Figure 17 gives the results of the testing for the boron/aluminum composite material. Again, as was the case for the graphite/epoxy, the boron/aluminum appeared to be insensitive to fatigue at the lower stress levels. At a stress level of approximately 50 ksi, the specimens would not fail at the high level of  $10^5$  cycles and greater. In one case, one of the composite specimens failed at a static load of about 52 ksi before starting the test. Based on these results, the two composite materials appear to not have a fatigue problem when loaded in tension.

The fatigue results for the 410 stainless steel in the annealed condition is shown in Figure 18. As expected, the curve for the machined crack specimens is lower by about 12 ksi than for the machined hole specimens for similar cycle values. The slope of the curves for the machined crack and hole specimens was very similar.

The fatigue results for the 410 stainless steel in the heat-treated condition is shown in Figure 19. Again, as expected, the curve for machined crack specimens was lower than for the machined hole specimens; however, the slope for the specimens with the crack was much greater in value than for the specimen with the hole. This difference in the slope

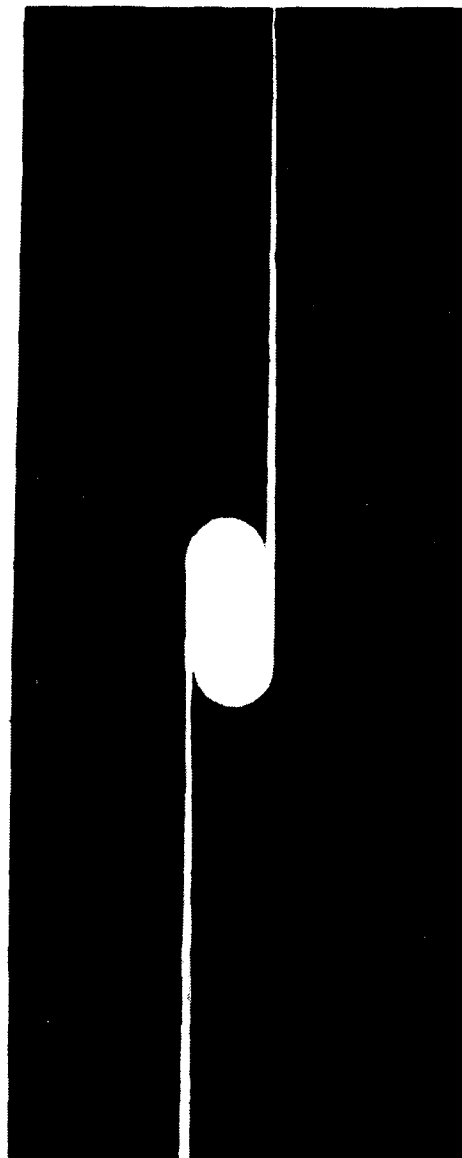


Figure 22. Longitudinal Cracks Developed on Graphite/  
Epoxy Specimen Upon Dynamic Load Application  
in Fatigue Testing

appears to indicate that the heat-treated specimens with the machined crack are appreciately more sensitive to fatigue than the specimens with machined hole. This large difference in the value of the slope for the machined crack and hole specimens occurred only for this material. The other metal materials all had similar slopes for their specimens with cracks and holes.

Figure 20 shows the fatigue results for the 6-4 titanium specimens. Again, the curve for the machined crack specimens is lower than for the machined hole specimens by about 33 ksi for the same number of cycles.

The fatigue results for the 8-1-1 titanium material was very similar to the 6-4 titanium specimens as shown in Figure 21. The spread in the curve for the machined crack specimens was about 33 ksi lower than for the machined hole specimens.

#### 3.4.1 Rating of the Materials for the Fatigue Tests

The rating of the materials for the fatigue testing was achieved by determining the stress levels of the various materials at the  $10^4$  and  $10^5$  cycle levels. The best material would be that which has the highest stress levels for the two cycle levels. Table 9 gives the stress levels at the two cycle levels for each material. The data for the material was off-scale; however, the values were obtained by extrapolation.

Based on this information, it appears that the composite material response to the fatigue tests was that failure would appear early under the high stress levels and no failure under the lower stress levels. In one case, for a boron/aluminum machined hole specimen, the specimen failed while the static load was being applied and before the test was actually started. Thus, the specimens appeared to fail due to the high tensile load rather than the dynamic cycling of the loads. For the graphite/epoxy machined crack specimens, longitudinal cracks occurred when the dynamic loads were applied and continued to grow until the test was stopped. The stress

TABLE 9  
STRESS VALUES OF FATIGUE TESTS AT  $10^4$   
AND  $10^5$  CYCLES FOR EACH MATERIAL

Test Material	Stress (psi) at $10^4$ Cycles Crack	Stress (psi) at $10^4$ Cycles Hole	Stress (psi) at $10^5$ Cycles Crack	Stress (psi) at $10^5$ Cycles Hole	Rating of Materials Crack	Rating of Materials Hole
Graphite/Epoxy	$\sim 105 \times 10^3$	$\sim 110 \times 10^3$	$83 \times 10^3$	$72 \times 10^3$	10.0	10.0
Boron/Aluminum	$\sim 50 \times 10^3$	$\sim 50 \times 10^3$	$\sim 50 \times 10^3$	$\sim 50 \times 10^3$	5.3	5.5
410 SS (Annealed)	$55 \times 10^3$	$67 \times 10^3$	$31 \times 10^3$	$44 \times 10^3$	4.6	6.1
410 SS (Heat Treated)	$86 \times 10^3$	$103 \times 10^3$	$\sim 28 \times 10^3$	$69 \times 10^3$	6.1	9.5
6-4 Ti	$54 \times 10^3$	$87 \times 10^3$	$20 \times 10^3$	$50 \times 10^3$	3.9	7.5
8-1-1 Ti	$50 \times 10^3$	$85 \times 10^3$	$23 \times 10^3$	$56 \times 10^3$	3.9	7.7

values for the graphite/epoxy composite specimens were greater than 100 ksi for the  $10^4$  cycle value and greater than 70 ksi for the  $10^5$  cycle value. Thus, the graphite/epoxy material was clearly the best material in resistance to fatigue and assigned a ranking of ten. For the  $10^4$  cycle value, the material had a stress level of 105 ksi for the specimens with a crack and a level of 110 ksi for the specimens with a hole. For the  $10^5$  cycle value, stress levels of 83 and 72 ksi were received for the crack and hole specimens, respectively. Based on this information, the remaining materials were ranked by addition of the stress levels for a particular material divided the total for the best material times ten. Thus, the equation for specimens with a crack is:

$$\text{Fatigue Rank} = \frac{\text{stress level total for both cycle values}}{188} \times 10.$$

The equation for the hole specimens is:

$$\text{Fatigue Rank} = \frac{\text{stress level total for both cycle values}}{182} \times 10.$$

The boron/aluminum material had a constant stress level of 50 ksi for both cycle levels and specimen types. Based on the ranking system, the rank for the crack specimens is 5.3 and 5.5 for the hole specimens.

The 410 stainless steel material in the annealed condition did not fare too well in the fatigue tests and received the lowest rating for the metal materials. For the  $10^4$  cycle value, the material had a stress level of 55 ksi for the specimens with a crack and a level of 57 ksi for the specimens with a hole. For the  $10^5$  cycle value, stress levels of 31 and 44 ksi were received for the crack and hole specimens, respectively. Using the ranking system, ratings of 4.6 and 6.1 were received for the crack and hole specimens, respectively.

The 410 stainless steel material in the heat-treated condition showed a marked improvement in fatigue strength compared to the annealed specimens. For the  $10^4$  cycle value,

stress levels of 86 and 103 ksi were received for the crack and hole specimens, respectively. A stress level of about 28 ksi was received for the crack specimens for the cycle level of  $10^5$  and 69 ksi for the hole specimens. Those heat-treated specimens exhibited the best response to fatigue of any of the metal materials. The material also appeared to be insensitive to fatigue for the hole specimens and somewhat sensitive to fatigue for specimens with a crack. Using the ranking system, a rating of 6.1 is received for the crack specimens and 9.5 for the hole specimens.

The 6-4 and 8-1-1 titanium materials exhibited a very similar response to fatigue. For the 6-4 titanium material, stress levels for the crack specimens of 54 and 20 ksi were received for the  $10^4$  and  $10^5$  cycle levels, respectively. For the specimens with a hole, stress levels at the  $10^4$  and  $10^5$  cycle values were 87 and 50 ksi, respectively. Based on the ranking system, ratings of 3.9 and 7.5 are received for the crack and hole specimens, respectively.

The 8-1-1 titanium had stress levels of 50 and 23 ksi for the crack specimens at the cycle levels of  $10^4$  and  $10^5$ , respectively. The stress levels for the hole specimens was 85 and 56 ksi at the  $10^4$  and  $10^5$  cycle levels, respectively. Based on this information, ratings of 3.9 and 7.7 are received for the crack and hole specimens, respectively.

Table 10 presents the average rating for the various materials investigated in the fatigue tests. The results indicated that the graphite/epoxy material displayed the best response to fatigue. The best metal material was the 410 stainless steel in the heat-treated condition followed by the titanium materials. The worst material in the fatigue tests was the 410 stainless steel in the annealed condition. The boron/aluminum composite material appeared to have an endurance limit at all cycle levels of about 50 ksi.

TABLE 10  
RANKING OF MATERIALS  
FOR FATIGUE TESTS

Test Material	Overall Average Rating
Graphite/Epoxy	10.00
Boron/Aluminum	5.40
410 SS (Annealed)	5.35
410 SS (Heat Treated)	7.80
6-4 Ti	5.70
8-1-1 Ti	5.80

#### 3.4.2 Evaluation of the Fatigue Test

The fatigue test appears to be an excellent screening method to rank candidate materials when damage is likely to be in the form of perforations or cracks generated at the impact site for FOD impacts.

#### 3.5 OVERALL RANKING OF THE MATERIALS TO THE SCREENING TESTS

The ranking of the materials is summarized in Table 11 for all of the screening tests. Based on these results, the best rating by averaging the rating of all the screening tests is given to 8-1-1 titanium followed closely by the 6-4 titanium material. The 8-1-1 titanium material exhibited very good results compared to that of the other materials evaluated except for the fatigue tests of the specimens with a crack. The 410 heat-treated stainless steel material gave good results in every screening test; and its lowest rating of 5.1 was received in the plastic deformation.

The 410 stainless steel material in the annealed condition had the lowest rating results for the metals; however, its rating is above that for the composite materials.

TABLE 11  
RANK OF THE MATERIALS FOR ALL THE SCREENING TESTS

Material	Overall Rank (Rating Average)	Material Ratings for Individual Screening Tests			
		Ballistic Limit Test	Plastic Deformation Test	Charpy Tests	Fatigue Tests
8-1-1 Ti	1(8.6)	8.5	10.0	10.00	5.80
6-4 Ti	2(8.3)	8.5	10.0	9.05	5.70
410 SS (Heat Treated)	3(7.9)	10.0	5.1	8.75	7.80
410 SS (Annealed)	4(5.8)	10.0	3.7	4.30	5.35
Graphite/Epoxy	5(4.4)	0.7	1.1	4.30	10.00
Boron/Aluminum	6(3.3)	1.9	3.4	2.65	5.40



The graphite/epoxy composite material exhibited very poor response to all the screening tests except for the fatigue tests. It appeared that the graphite/epoxy was insensitive to fatigue at the lower stress levels and it had the highest rating for the fatigue tests. The graphite/epoxy appeared to be slightly better than the boron/aluminum material when considering all of the screening tests. In the screening tests, the boron/aluminum material ratings were poor in every case. The highest rating of 5.4 was received in the fatigue tests.

## SECTION IV

### SUMMARY AND CONCLUSIONS

A number of general conclusions may be drawn from the data generated in this study. Several material screening tests to effectively evaluate and rank the response of candidate materials to impact of fan and compressor blades were investigated. The material parameters that were investigated in this study include: (a) the perforation resistance of the materials; (b) the extent the material may plastically deform; (c) the extent to which the material is vulnerable to catastrophic structural failure; and (d) the extent to which the material is vulnerable to degradation of fatigue properties. The conclusions for the various material parameters investigated in the study are given in the following paragraphs.

#### 4.1 BALLISTIC LIMIT TESTS

The perforation resistance material parameter was quantified as a ballistic limit velocity for a given impact condition. Results of the ballistic limit testing for the three impactors (pebble, artificial bird, and ice ball) utilized on six candidate materials (410 stainless steel in the annealed condition, 410 stainless steel in the heat-treated condition, 8-1-1 titanium, 6-4 titanium, boron/aluminum composite, and a graphite/epoxy composite) indicated that the pebble impacts were the only ones which could be considered for the metal specimens. Non-penetrations were received by the metal specimens for the artificial bird and ice ball impacts. Both alloys of 410 stainless steel was superior compared to the other materials in resistance to perforation. Both composite materials exhibited very poor perforation resistance to the pebble and artificial bird impacts. The mode of failure for the metal materials and the boron/aluminum material for the pebble impacts was in the form of either petaling or plugging. The mode of failure for

the substitute bird impacts on the graphite/epoxy material was cracking and splitting through the entire length of the specimens due to the fact it was an unidirectional laminate.

The equation used to rate the various materials was:

$$V_L = \frac{\text{material ballistic limit}}{1020} \times 10.$$

The constant of 1020 is the ballistic limit of the stainless steel materials which was superior in the test.

The ballistic limit tests is an excellent screening test of candidate materials; however, careful considerations must be made in selecting the projectile type and material to receive perforations for each material investigated.

#### 4.2 PLASTIC DEFORMATION TESTS

The plastic deformation material parameter was quantified by conducting ballistic tests which maximized the likelihood of plastic deformation. A slight amount of plastic deformation occurring from impacts may be considered relatively benign for fan and compressor blades; however, a large amount would effect the aerodynamic performance of the system. A combination of elastic and plastic deformation could be sufficiently large enough to cause blade contact with static structural components causing catastrophic failure of the blade and engine.

Again, the pebble impacts were used to rate the materials in resistance to plastic deformation. The substitute bird impacts on the graphite/epoxy material indicated that it failed to deform plastically up to velocities of 97 m/s which is its ballistic limit. The titanium materials was superior compared to the other materials for the plastic deformation test. The heat-treated stainless steel was rated below the titanium followed by the annealed stainless steel alloy. The boron/aluminum was rated slightly better than the graphite/epoxy composite.

The equation used to rate the various materials was:

$$PD_R = \frac{\text{material impact velocity}}{\text{plastic deformation}} \times \frac{3.6}{855} \times 10.$$

The constants of 3.6 and 855 are the plastic deformation and velocity values of the 8-1-1 titanium material, respectively.

The plastic deformation test is an excellent screening test of candidate materials; however, careful considerations must again be taken in selecting the projectile type and material to receive maximum deformations for each material investigated.

#### 4.3 GROSS STRUCTURAL DAMAGE TESTS

The material response of the six materials to bending stresses was investigated by using the instrumented charpy impact test. The force and energy level required to break a standard thickness specimen was used to rate the various materials. Based on the results of the testing, the 8-1-1 titanium was superior followed closely by the 6-4 titanium. The 410 stainless steel in the heat-treated condition also exhibited good response and was rated third. The remaining three materials (the annealed 410 stainless steel, the graphite/epoxy and the boron/aluminum) demonstrated poor response to the charpy impact test. The stainless steel material was ranked fourth followed by the graphite/epoxy and then the boron/aluminum material. A substantial amount of yielding was experienced for the metal specimens and very little for the composite specimens. The composite materials would fail almost instantly without yielding once the peak force was reached.

The equations used to rate the various materials were:

$$\text{Peak Force} = \frac{\text{force of material}}{183.2} \times 10$$

for the peak force and:

$$\text{Peak Energy} = \frac{\text{energy level of material}}{9.00} \times 10$$

for the peak energy level.

The instrumented charpy impact test is an excellent test to screen candidate materials to resist bending. It is a test that would be used where large bird impacts are anticipated to generate gross bending at the impact site and the root.

#### 4.4 FATIGUE TESTS

The fatigue properties parameter of the six materials investigated was quantified in terms of the ultimate tensile fatigue strength of damaged specimens with machined holes and cracks in the center of the specimens at their midspan. The damaged specimens were fatigue tested in tension to obtain the number of cycles till failure (complete separation).

The ranking of the materials was achieved by determining the stress levels of the various materials at the  $10^4$  and  $10^5$  cycle levels. The best material was the graphite/epoxy composite material. The composite specimens more or less failed due to the high tensile loads rather than the dynamic cycling of the loads. The best metal material was the 410 stainless steel in the heat-treated condition. This material appeared to be insensitive to fatigue for specimens with a hole and somewhat sensitive to fatigue for specimens with a crack.

The 8-1-1 and 6-4 titanium materials exhibited a very similar response to fatigue and were ranked below the 410 stainless steel material in the heat-treated state. The 410 stainless steel in the annealed condition exhibited the lowest fatigue results and was ranked last in the fatigue testing.

The equation used to rate the various material specimens with a crack was:

$$\text{Fatigue Rank} = \frac{\text{stress level for both cycle levels}}{188} \times 10.$$

The equation used to rate the various material specimens with a hole was:

$$\text{Fatigue Rank} = \frac{\text{stress level for both cycle levels}}{182} \times 10.$$

The constants of 188 and 182 are the stress level totals of the graphite/epoxy material for the crack and hole specimens, respectively.

The fatigue test appeared to be an excellent screening method to rate candidate materials when the damage is in the form of perforations or cracks generated at the impact site for FOD impacts.

#### 4.5 OVERALL RANKING OF THE MATERIALS TO THE SCREENING TESTS

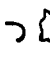







The best material by averaging the rating of all the screening tests was the 8-1-1 titanium followed closely by the 6-4 titanium alloy. The 8-1-1 titanium material exhibited good response in every screening test except for the fatigue tests of the specimens with a crack. The heat-treated stainless steel material received good ratings in every test with a lowest rating of 5.1 in the plastic deformation test and the fatigue test of specimens with a crack. This material was ranked third behind the titanium alloys.

The 410 stainless steel material in the annealed condition had the lowest rating results for the metals; however, its average rating for all the tests was above that for the composite materials.


The graphite/epoxy composite material exhibited very poor response to all the screening tests except for the fatigue tests where it had the best response of all the materials. The ranking of the graphite/epoxy material was below the metals and above the boron/aluminum material.

The boron/aluminum composite material was ranked last of all the materials and displayed poor response in all of the screening tests. In the fatigue tests, it appeared to have a constant endurance limit of 50 ksi for both cycle levels and specimen type.







APPENDIX  
TEST RESULTS

SHOT	MATERIAL	SIZE (cm)	IMPACT ANGLE	SUPPORT METHOD	PROJECTILE TYPE SIZE (cm)	MASS (grams)	VELOCITY (m/s)	RESULTS	DEFORM- ATION (cm)	CRACK LENGTH (cm)	SKETCH	HOLE DIA. (cm)
3-0081	410SS ANNEALED	7.62X7.62X.16	90°	SIMPLE METHOD	PEBBLE .64		898	BULGE	1.31			
3-0082	410SS ANNEALED	7.62X7.62X.16	90°	SIMPLE METHOD	PEBBLE .64		1052	BULGE AND CRACK	1.42	.89		
3-0083	410SS ANNEALED	7.62X7.62X.16	90°	SIMPLE METHOD	PEBBLE .64		1341	COMPLETE PENETRATION SPECIMEN PETAILED				2.03
3-0084	410SS ANNEALED	7.62X7.62X.16	90°	SIMPLE METHOD	PEBBLE .64		1252	COMPLETE PENETRATION SPECIMEN PETAILED				2.03
3-0085	410SS ANNEALED	7.62X7.62X.16	90°	SIMPLE METHOD	PEBBLE .64		1104	MULTIPLE IMPACTS PEBBLE BROKE UP BEFORE IMPACT	1.23			
3-0086	410SS ANNEALED	7.62X7.62X.16	90°	SIMPLE METHOD	PEBBLE .64	.4256	1039	COMPLETE PENETRATION SPECIMEN PETAILED				1.02
3-0087	410SS ANNEALED	7.62X7.62X.16	90°	SIMPLE METHOD	PEBBLE .64	.3945	1147	COMPLETE PENETRATION SPECIMEN PETAILED				1.27
3-0088	410SS ANNEALED	7.62X7.62X.16	90°	SIMPLE METHOD	PEBBLE .64	.4143	1071	BULGE	1.25			
3-0089	410SS HEAT TREATED	7.62X7.62X.16	90°	SIMPLE METHOD	PEBBLE .64	.3920	1077	BULGE-PEBBLE BROKE UP BEFORE IMPACT	.76			.81
3-0090	410SS HEAT TREATED	7.62X7.62X.16	90°	SIMPLE METHOD	PEBBLE .64	.3932	1022	COMPLETE PENETRATION STARTED TO PETAL				
3-0091	410SS HEAT TREATED	7.62X7.62X.16	90°	SIMPLE METHOD	PEBBLE .64	.4035	941	BULGE	.78			
3-0093	410SS HEAT TREATED	7.62X7.62X.16	90°	SIMPLE METHOD	PEBBLE .64	.4130	1027	COMPLETE PENETRATION STARTED TO PETAL		.33		
3-0100	410SS ANNEALED	7.62X7.62X.16	90°	SIMPLE METHOD	PEBBLE .64	.4007	988	COMPLETE PENETRATION SPECIMEN PETAILED				.89
3-0101	410SS ANNEALED	7.62X7.62X.16	90°	SIMPLE METHOD	PEBBLE .64	.3847	935	BULGE	.86			



SHOT	MATERIAL	SIZE (cm)	IMPACT ANGLE METHOD	PROJECTILE TYPE SIZE (cm)	MASS (grams)	VELOCITY (m/s)	RESULTS	DEFOR- MATION (cm)	CRACK LENGTH (cm)	SKETCH	HOLE DIA. (cm)
3-0102	410SS ANNEALED	7.62X7.62X.16	90° SIMPLE METHOD	PEBBLE .64	.3700	961	BULGE	.88			
3-0103	410SS ANNEALED	7.62X7.62X.16	90° SIMPLE METHOD	PEBBLE .64	.3830	1010	BULGE	1.0			
3-0104	410SS ANNEALED	7.62X7.62X.16	90° SIMPLE METHOD	PURBLE .64	.3817	1004	COMPLETE PENETRATION SPECIMEN PETALLED				.96
3-0105	410SS ANNEALED	7.62X7.62X.16	90° SIMPLE METHOD	PEBBLE .64	.3703	916	BULGE	.96			
3-0106	410SS ANNEALED	7.62X7.62X.16	90° SIMPLE METHOD	PEBBLE .64	.3835	1027	BULGE	1.35			
3-0107	410SS ANNEALED	7.62X7.62X.16	90° SIMPLE METHOD	PEBBLE .64	.3825	1039	BULGE	1.25			
3-0135	410SS ANNEALED	7.62X7.62X.16	90° SIMPLE METHOD	MICRO BALLOON 1.27	.9520	496	BULGE	.41			
3-0136	410SS ANNEALED	7.62X7.62X.16	90° SIMPLE METHOD	MICRO BALLOON 1.27	.9850	528	BULGE	.47			
3-0137	410SS ANNEALED	7.62X7.62X.16	90° SIMPLE METHOD	MICRO BALLOON 1.27	.9865	606	BULGE	.56			
3-0138	410SS ANNEALED	7.62X7.62X.16	90° SIMPLE METHOD	ICE BALL 1.27	1.1046	606	BULGE	.34			
3-0139	410SS ANNEALED	7.62X7.62X.16	90° SIMPLE METHOD	ICE BALL 1.27	.8972	621	BULGE	.37			
3-0140	410SS ANNEALED	7.62X7.62X.16	90° SIMPLE METHOD	MICRO BALLOON 1.27	1.0284	918	BULGE	.56			
3-0154	410SS ANNEALED	7.62X7.62X.16	90° SIMPLE METHOD	MICRO BALLOON 1.27	.9200	593	BULGE	.33			
3-0155	410SS ANNEALED	7.62X7.62X.16	90° SIMPLE METHOD	MICRO BALLOON 1.27	.9500	597	BULGE	.29			

SHOT	MATERIAL	SIZE (cm)	IMPACT SUPPORT ANGLE METHOD	PROJECTILE TYPE SIZE (cm)	MASS (grams)	VELOCITY (m/s)	RESULTS	DEFOR- MATION (cm)	CRACK LENGTH (cm)	SKETCH	HOLE DIA. (cm)
3-0127	B/A1	7.62X7.62X.16	90° SIMPLE METHOD	MICRO BALLOON 1.27	1.0216	315	COMPLETE PENETRATION		2.858		1.60
3-0128	B/A1	7.62X7.62X.16	90° SIMPLE METHOD	MICRO BALLOON 1.27	.9900	379	COMPLETE PENETRATION		1.905		
3-0129	B/A1	7.62X7.62X.16	90° SIMPLE METHOD	MICRO BALLOON 1.27	1.0190	301	COMPLETE PENETRATION BULGE AND CRACK STARTED TO PETAL	.803	1) 2.01 2) 2.03 3) 4.95		
3-0130	B/A1	7.62X7.62X.16	90° SIMPLE METHOD	MICRO BALLOON 1.27	.9932	291	COMPLETE PENETRATION BULGE AND CRACK	.538	3.747		
3-0131	B/A1	7.62X7.62X.16	90° SIMPLE METHOD	MICRO BALLOON 1.27	1.0123	270	COMPLETE PENETRATION BULGE AND CRACK	.541	4.191		
3-0132	B/A1	7.62X7.62X.16	90° SIMPLE METHOD	MICRO BALLOON 1.27	1.00	257	COMPLETE PENETRATION BULGE AND CRACK	.455	3.175		
3-0133	B/A1	7.62X7.62X.16	90° SIMPLE METHOD	MICRO BALLOON 1.27	1.00	217	BULGE AND SLIGHT CRACK	.241			
3-0134	B/A1	7.62X7.62X.16	90° SIMPLE METHOD	MICRO BALLOON 1.27	1.0066	236	BULGE AND SLIGHT CRACK	.368	2.235		
3-0151	Ti 8-1-1	7.62X7.62X.16	90° SIMPLE METHOD	PEBBLE .635	.3782	982	COMPLETE PENETRATION SPECIMEN PETAELED				1.52
3-0152	Ti 8-1-1	7.62X7.62X.16	90° SIMPLE METHOD	PEBBLE .635	.3773	854	BULGE	.36			
3-0153	Ti 8-1-1	7.62X7.62X.16	90° SIMPLE METHOD	PEBBLE .635	.3800	889	COMPLETE PENETRATION STARTED TO PETAL	.58	2.16		

SHOT	MATERIAL	SIZE (cm)	IMPACT ANGLE METHOD	PROJECTILE TYPE SIZE (cm)	MASS (grams)	VELOCITY (m/s)	RESULTS	DEFORM- MATION (cm)	CRACK LENGTH (cm)	SKETCH	SOLE DIA. (cm)
3-0097	B/A1	7.62X7.62X.16	90° SIMPLE METHOD	PEBBLE .635	.40	216	COMPLETE PENETRATION BULGE AND CRACK STARTED TO PLUG	.155	.483		.483
3-0098	B/A1	7.62X7.62X.16	90° SIMPLE METHOD	PEBBLE .635	.4050	208	COMPLETE PENETRATION BULGE AND CRACK STARTED TO PLUG	.315	.381		.432
3-0099	B/A1	7.62X7.62X.16	90° SIMPLE METHOD	PEBBLE .635	.3885	178	PARTIAL PENETRATION BULGE AND CRACK STARTED TO PLUG	.198			.508
3-0108	B/A1	7.62X7.62X.16	90° SIMPLE METHOD	PEBBLE .635	.3770	200	COMPLETE PENETRATION BULGE AND CRACK STARTED TO PLUG	.254			.406
3-0109	B/A1	7.62X7.62X.16	90° SIMPLE METHOD	PEBBLE .635	.4003	185	PARTIAL PENETRATION BULGE AND CRACK STARTED TO PLUG	.231			.33
3-0120	B/A1	7.62X7.62X.16	90° SIMPLE METHOD	MICRO BALLOON 1.27	.8878	179	NO DAMAGE				
3-0121	B/A1	7.62X7.62X.16	90° SIMPLE METHOD	MICRO BALLOON 1.27	.8900	191	NO DAMAGE				
3-0122	B/A1	7.62X7.62X.16	90° SIMPLE METHOD	MICRO BALLOON 1.27	.9900	304	COMPLETE PENETRATION BULGE WITH CRACKS STARTED TO PETAL	.658	1) 1.65 2) 1.14 3) 5.055		
3-0123	B/A1	7.62X7.62X.16	90° SIMPLE METHOD	MICRO BALLOON 1.27	.9935	252	BULGE	.160			
3-0124	B/A1	7.62X7.62X.16	90° SIMPLE METHOD	MICRO BALLOON 1.27	.9958	312	SLIGHT BULGE				
3-0125	B/A1	7.62X7.62X.16	90° SIMPLE METHOD	MICRO BALLOON 1.27	.9853	297	BULGE AND CRACK	.368	2.54		
3-0126	B/A1	7.62X7.62X.16	90° SIMPLE METHOD	MICRO BALLOON 1.27	.9964	304	COMPLETE PENETRATION		2.54		1.52

SHOT	MATERIAL	SIZE (cm)	IMPACT SUPPORT ANGLE METHOD	PROJECTILE TYPE SIZE (cm)	MASS (grams)	VELOCITY (m/s)	RESULTS	DEFOR- MATION (cm)	CRACK LENGTH (cm)	SKETCH	HOLE DIA. (cm)
3-0156	Ti 6-4	7.62X7.62X.16	90° SIMPLE METHOD	MICRO BALLOON 1.27	.9332	586	SLIGHT BULGE	.28			
3-0157	Ti 6-4	7.62X7.62X.16	90° SIMPLE METHOD	MICRO BALLOON 1.27	.9612	585	SLIGHT BULGE	.28			
3-0158	Ti 8-1-1	7.62X7.62X.16	90° SIMPLE METHOD	MICRO BALLOON 1.27	.9763	598	SLIGHT BULGE	.26			
3-0159	Ti 8-1-1	7.62X7.62X.16	90° SIMPLE METHOD	MICRO BALLOON 1.27	.9532	580	BULGE	.2			
3-0160	Ti 8-1-1	7.62X7.62X.16	90° SIMPLE METHOD	ICE BALL 1.27	.9700		BAD SHOT MISSED TARGET				
3-0161	Ti 8-1-1	7.62X7.62X.16	90° SIMPLE METHOD	ICE BALL 1.27	.9657	573	SLIGHT BULGE	.046			
3-0162	Ti 8-1-1	7.62X7.62X.16	90° SIMPLE METHOD	ICE BALL 1.27	.9657	663	SLIGHT BULGE	.038			

SHOT	MATERIAL	SIZE (cm)	IMPACT SUPPORT ANGLE METHOD	PROJECTILE TYPE SIZE (cm)	MASS (grams)	VELOCITY (m/s)	REMARKS
3-0146	G/EP	7.62X7.62X.16	90° SIMPLE METHOD	MICRO BALLOON 1.27	1.0010	129	SPECIMEN BROKE FIVE PIECES
3-0147	G/EP	7.62X7.62X.16	90° SIMPLE METHOD	MICRO BALLOON 1.27	1.0034	99	SPECIMEN BROKE TWO PIECES
3-0148	G/EP	7.62X7.62X.16	90° SIMPLE METHOD	MICRO BALLOON 1.27	1.0111	74	NO DAMAGE
3-0149	G/EP	7.62X7.62X.16	90° SIMPLE METHOD	MICRO BALLOON 1.27	1.0052	86	NO DAMAGE
3-0150	G/EP	7.62X7.62X.16	90° SIMPLE METHOD	MICRO BALLOON 1.27	1.0167	95	NO VISUAL DAMAGE

## SECTION V

### REFERENCES

1. Krinke, D. C., Barber, J. P., and Nicholas, T., "The Charpy Impact Test As a Method for Evaluating Impact Resistance of Composite Materials," Technical Report for Air Force Materials Laboratory, AFML-TR-78-54, April 1978.
2. Peterson, R. E., "Stress Concentration Design Factors," John Wiley and Sons Inc., 1953.

TE  
MED